4. Transfer 2 μL of 2 mg/mL RNA to a new tube and add 8 μL of sample buffer, then incubate at 65°C for 15 min and transfer onto ice.
5. Spin the tube down briefly, add 2 μL of gel-loading buffer, and apply the sample to a denaturing agarose gel.
6. After electrophoresis, rinse the agarose gel with DEPC-treated water once for 10 min with gentle shaking.
7. For a minigel, incubate in 150 mL of 50 mM NaOH/10 mM NaCl solution at room temperature for 20 min.
8. Discard the solution and rinse the gel with DEPC-treated water.
9. Incubate in 150 mL of 0.1 M Tris-HCl, pH 7.4, at room temperature for 20 min.
10. Discard the solution and rinse the gel with DEPC-treated water.
11. Incubate in 150 mL of 20× SSC at room temperature for 20 min.
12. Transfer the gel onto a Hybond-N+ membrane at 50–55 cm H_2O for 1 h (*see* **Note 4**).
13. Immobilize the membrane using a Stratalinker™ UV crosslinker.
14. Purify the DNA fragment containing the *NS3* to *5B* genes of JFH-1.
15. Transfer 25 ng of the purified DNA fragment into a new tube and add 5 μL of primer solution from the Megaprime™ DNA labeling system and distilled water to a total volume of 33 μL.
16. Boil the solution for 5 min and then transfer it onto ice.
17. Add 10 μL of labeling buffer and 5 μL of [α−^{32}P]dCTP, followed by 2 μL of enzyme solution, and then incubate the mixture at 37°C for 10 min.
18. Purify the [α−^{32}P]dCTP-labeled DNA probe using a S-300HR spin column.
19. Determine the specific activity with a scintillation counter.
20. Incubate the membrane with 0.125 mL/cm^2 Rapid-Hyb Buffer™ at 65°C for at least 15 min. During this incubation period, boil the probe for 5 min and then place it on ice for 2 min.
21. Add the boiled probe at 1 ×10^5 cpm/mL buffer and incubate at 65°C for 2 h with shaking.
22. Wash the hybridized membrane with 2 × SSC/0.1% SDS at room temperature for 10 min three times.
23. Wash the membrane with 1 × SSC/0.1% SDS at 65°C for 15 min once.
24. Wash the membrane with 0.1 × SSC/0.1% SDS at 65°C for 20 min three times.
25. Expose the membrane to X-ray film.

3.12. Quantification of HCV Core Protein

For estimation of levels of HCV core protein in culture supernatant or cell lysate, concentrations of HCV core protein can be determined by HCV core protein immunoassay. Cell pellets can be lysed in lysis buffer.

1. Dilute the HCV core standard solution with standard diluent and prepare 3600, 1200, 400, 133, and 44.4 fmol/L solutions. Use standard diluent as a negative control (0 fmol/L).
2. Add 50 μL of pretreatment solution to 100 μL of sample and mix (*see* **Note 5**).
3. Incubate at 56–60°C for 30 min and then at room temperature for 5 min.
4. Determine the number of eight-well strips needed for the assay. Insert these into the frame for current use.
5. Add 100 μL of reaction buffer to each well.
6. Add 100 μL of each standard solution and pretreated samples to the appropriate wells. Mix them by pipetting.
7. Cover the plate with a plate cover and incubate it for 60 min at room temperature with shaking on a plate mixer.
8. Thoroughly aspirate or decant solution from the wells and discard the liquid. Take care not to scratch the inside of the well. After aspiration, fill the wells with wash solution, being careful not to overflow the wells. Soak for at least 20 s and then aspirate the liquid. Repeat this washing procedure six times.
9. Add 200 μL of labeled-antibody solution to each well.
10. Cover the plate with a plate cover and incubate it for 30 min at room temperature.
11. Thoroughly aspirate or decant solution from the wells and discard the liquid. Wash the wells six times as described above.
12. Add 200 μL of substrate solution to each well. Incubate for 30 min at room temperature in the dark.
13. Add 50 μL of stop solution to each well. Tap the side of the plate gently to mix.
14. Read the absorbance of each well at 492 nm against two negative control wells.
15. Plot the absorbance of each standard against the standard concentration. Draw the best smooth curve through these points to construct the standard curve.
16. Determine HCV core protein concentrations for unknown samples from the standard curve. Samples with concentrations exceeding the highest standard (3600 fmol/L) should be diluted and reanalyzed. Samples producing less than 100 fmol/L should also be reanalyzed for confirmation of results.
17. Determine the total lysate protein concentrations, for example using the Bradford method, and adjust them to 1 mg/mL with normal serum. HCV core protein concentrations within

cell lysate can be expressed as fmol/g of total protein when divided by total protein concentrations (*see* **Note 6**).

3.13. Quantification of HCV RNA by Real-Time RT-PCR

Copy numbers of HCV RNA in culture supernatant or infected cells can be determined by real-time detection RT-PCR (RTD-PCR), using TaqMan EZ RT-PCR Core Reagents kit and the 7500 Real-Time PCR System.

1. To synthesize standard RNA for quantification, prepare plasmid DNA containing the HCV IRES sequence.
2. Synthesize an HCV RNA standard using an appropriate commercial kit, such as the MEGAscript™ T7 kit. Check the integrity of the synthesized RNA by denaturing agarose gel electrophoresis as described above.
3. Determine RNA concentrations by measuring optical density at OD260 and OD280. Calculate the copy number of synthesized RNA from the concentration and length of RNA. Adjust the standard RNA concentration to 10^{10} copies/μL with nuclease-free water.
4. Prepare primers and the TaqMan probe listed in **Table 23.2**.
5. Dilute HCV RNA standard solution with RNA standard dilution buffer and prepare 10^7, 10^6, 10^5, 10^4, 10^3, 10^2, and 10^1 copies/μL E solutions. Use nuclease-free water as a negative control.
6. Prepare the reaction mixture as follows:

Nuclease-free water	7.1 μL
5× TaqMan EZ buffer	5 μL
10 mM dATP	0.5 μL
10 mM dGTP	0.5 μL
10 mM dCTP	0.5 μL
20 mM dUTP	0.65 μL
10 μm 130S primer	0.5 μL
10 μm 290R primer	0.5 μL
3 μm TaqMan probe	2.5 μL
25 mM $Mn(OAc)_2$	3 μL
AmpErase UNG	0.25 μL
rTth DNA polymerase	1.5 μL
Total	22.5 μL

7. Add 22.5 μL of reaction mixture to each well of the PCR plate.

Table 23.2
Primers and a probe used in RTD-PCR

Name	Sequence (5′ > 3′)
130S	5′- CGG GAG AGC CAT AGT GG-3′
290R	5′- AGT ACC ACA AGG CCT TTC G-3′
probe	5′- (6-Fam) CTG CGG AAC CGG TGA GTA CAC (Tamra) -3′

8. Add 2.5 μL of each RNA sample and standard to the appropriate wells. Use nuclease-free water as a negative control. All samples and controls should be evaluated in at least two wells.
9. Set the PCR plate in a 7500 Real-Time PCR System or an equivalent system.
10. Set the reaction conditions and incubate at 50°C for 2 min, 60°C for 30 min, 95°C for 5 min, followed by 50 cycles at 95°C for 20 s and 62°C for 1 min.
11. Confirm the absence of amplification in the negative control wells.
12. Determine RNA copy numbers in the samples using Sequence Detection Software.

3.14. Infection of Cells with Secreted HCV and Determination of Infectivity

1. Collect culture medium from RNA-transfected or infected cells.
2. Centrifuge the collected culture medium at 3000g for 20 min at 4°C, and pass the supernatant through a disk filter with a 0.45 μm pore size.
3. Concentrate the collected culture medium using an Amicon Ultra-15 device (100,000 MWCO) if necessary. Add up to 15 mL of culture medium to the upper chamber of the Amicon Ultra-15. Centrifuge at 3000g for 30 min at 4°C. The concentrated culture medium can be stored at −80°C until use.
4. Seed wells in poly-D-lysine-coated 96-well plates with Huh-7 cells at a density of 1×10^4 cells on the day before virus inoculation.
5. Dilute culture medium containing infectious JFH-1 virus.
6. Discard the culture medium from the plates seeded with Huh-7 cells.
7. Add 100 μL of serially diluted virus solution to at least six wells per dilution, and incubate for 4 h at 37°C.
8. Remove the inoculum and add 100 μL of fresh complete medium, then incubate the inoculated cells for 72 h at 37°C under 5% CO_2.
9. At the end of incubation, remove the culture medium.
10. Fix the cells by dipping the plate into ice-chilled 100% methanol.

11. Incubate it at −20°C for 20 min.
12. Block the cells at room temperature for 1 h with 100 μL per well of blocking buffer, then wash with PBS(−) once.
13. Add 100 μL of anticore antibody solution to each well to make a concentration of 50 μg/mL in blocking buffer, and incubate at room temperature for 1 h.
14. Aspirate the antibody solution and wash the wells with PBS(−) three times.
15. Add 100 μL per well of AlexaFluor 488-conjugated anti-mouse IgG in blocking buffer, and incubate at room temperature for 1 h.
16. Aspirate the antibody solution and wash the wells with PBS(−) three times.
17. Count the stained cells using fluorescence microscopy.
18. Calculate the infectivity of the inoculum form the focus number and inoculum dilution, which can be expressed as focus-forming units per milliliter (ffu/mL). Alternatively, determine the TCID50 according to the method of Reed and Muench *(44)*.

4. Notes

1. The final concentration of formaldehyde is shown.
2. If the expected amount of recovered RNA is low, transfer RNA or glycogen should be added before isopropanol precipitation to enhance the precipitation efficiency.
3. If the 3′ residue might be A, other 3′ RACE methods should also be used, such as the linker ligation method.
4. The membrane should be rinsed with DEPC-treated water, then 20× SSC.
5. Multiple dilutions of samples may be necessary to produce core protein concentrations within a standard range. Fetal bovine serum can be used as the diluent.
6. Adjusting the total protein concentration may reduce background contamination.

Acknowledgments

This work was partially supported by a grant-in-aid for Scientific Research from the Japan Society for the Promotion of Science, from the Ministry of Health, Labour and Welfare of Japan, and from the Ministry of Education, Culture, Sports, Science and Technology and by the Research on Health Sciences Focusing on Drug Innovation from the Japan Health Sciences Foundation.

References

1. Bartenschlager, R. and Lohmann, V. (2001) Novel cell culture systems for the hepatitis C virus. *Antiviral Res.* **52,** 1–17.
2. Lohmann, V., Korner, F., Koch, J., Herian, U., Theilmann, L., and Bartenschlager, R. (1999) Replication of subgenomic hepatitis C virus RNAs in a hepatoma cell line. *Science* **285,** 110–113.
3. Blight, K. J., Kolykhalov, A. A., and Rice, C. M. (2000) Efficient initiation of HCV RNA replication in cell culture. *Science* **290,** 1972–1974.
4. Lohmann, V., Korner, F., Dobierzewska, A., and Bartenschlager, R. (2001) Mutations in hepatitis C virus RNAs conferring cell culture adaptation. *J. Virol.* **75,** 1437–1449.
5. Krieger, N., Lohmann, V., and Bartenschlager, R. (2001) Enhancement of hepatitis C virus RNA replication by cell culture-adaptive mutations. *J. Virol.* **75,** 4614–4624.
6. Ikeda, M., Yi, M., Li, K., and Lemon, S. M. (2002) Selectable subgenomic and genome-length dicistronic RNAs derived from an infectious molecular clone of the HCV-N strain of hepatitis C virus replicate efficiently in cultured Huh7 cells. *J. Virol.* **76,** 2997–3006.
7. Pietschmann, T., Lohmann, V., Kaul, A., Krieger, N., Rinck, G., Rutter, G., et al. (2002) Persistent and transient replication of full-length hepatitis C virus genomes in cell culture. *J. Virol.* **76,** 4008–4021.
8. Blight, K. J., McKeating, J. A., Marcotrigiano, J., and Rice, C. M. (2003) Efficient replication of hepatitis C virus genotype 1a RNAs in cell culture. *J. Virol.* **77,** 3181–3190.
9. Bukh, J., Pietschmann, T., Lohmann, V., Krieger, N., Faulk, K., Engle, R. E., et al. (2002) Mutations that permit efficient replication of hepatitis C virus RNA in Huh-7 cells prevent productive replication in chimpanzees. *Proc. Natl. Acad. Sci. USA* 99, 14416–14421.
10. Kato, T., Furusaka, A., Miyamoto, M., Date, T., Yasui, K., Hiramoto, J., et al. (2001) Analysis of hepatitis C virus isolated from a fulminant hepatitis patient. *J. Med. Virol.* **64,** 334–339.
11. Kato, T., Date, T., Miyamoto, M., Furusaka, A., Tokushige, K., Mizokami, M., et al. (2003) Efficient replication of the genotype 2a hepatitis C virus subgenomic replicon. *Gastroenterology* **125,** 1808–1817.
12. Uprichard, S. L., Chung, J., Chisari, F. V., and Wakita, T. (2006) Replication of a hepatitis C virus replicon clone in mouse cells. *Virol. J.* **3,** 89.
13. Date, T., Miyamoto, M., Kato, T., Morikawa, K., Murayama, A., Akazawa, D., et al. (2007) An infectious and selectable full-length replicon system with hepatitis C virus JFH-1 strain. *Hepatol. Res.* in press.
14. Kato, T., Date, T., Miyamoto, M., Sugiyama, M., Tanaka, Y., Orito, E., et al. Detection of anti-hepatitis C virus effects of interferon and ribavirin by a sensitive replicon system. *J. Clin. Microbiol.* **43,** 5679–5684.
15. Date, T., Kato, T., Miyamoto, M., Zhao, Z., Yasui, K., Mizokami, M., et al. (2004) Genotype 2a hepatitis C virus subgenomic replicon can replicate in HepG2 and IMY-N9 cells. *J. Biol. Chem.* **279,** 22371–22376.
16. Kato, T., Date, T., Miyamoto, M., Zhao, Z., Mizokami, M., and Wakita, T. (2005) Non-hepatic cell lines HeLa and 293 cells support efficient replication of hepatitis C virus genotype 2a subgenomic replicon. *J. Virol.* **79,** 592–596.
17. Wakita, T., Pietschmann, T., Kato, T., Date, T., Miyamoto, M., Zhao, Z., et al. (2005) Production of infectious hepatitis C virus in tissue culture from a cloned viral genome. *Nat. Med.* **11,** 791–796.
18. Zhong, J., Gastaminza, P., Cheng, G., Kapadia, S., Kato, T., Burton, D. R., et al. (2005) Robust hepatitis C virus infection in vitro. *Proc. Natl. Acad. Sci. USA* **102,** 9294–9299.
19. Blight, K. J., McKeating, J. A., and Rice, C. M. (2002) Highly permissive cell lines for subgenomic and genomic hepatitis C virus RNA replication. *J. Virol.* **76,** 13001–13014.
20. Sumpter, R., Jr., Loo, Y. M., Foy, E., Li, K., Yoneyama, M., Fujita, T., et al. (2005) Regulating intracellular antiviral defense and permissiveness to hepatitis C virus RNA replication through a cellular RNA helicase, RIG-I. *J. Virol.* **79,** 2689–2699.
21. Lindenbach, B. D., Evans, M. J., Syder, A. J., Wolk, B., Tellinghuisen, T. L., Liu, C. C., et al. (2005) Complete replication of hepatitis C virus in cell culture. *Science* **309,** 623–626.
22. Koutsoudakis, G., Herrmann, E., Kallis, S., Bartenschlager, R., and Pietschmann, T. (2007) The level of CD81 cell surface expression is a key determinant for productive entry of hepatitis C virus into host cells. *J. Virol.* 81, 588–598.
23. Akazawa, D., Date, T., Morikawa, K., Murayama, A., Miyamoto, M., Kaga, M., et al. (2007) CD81 expression is important for heterogeneous HCV permissiveness of Huh7 cell clones. *J. Virol.* [Epub ahead of print].

24. Nakabayashi, H., Taketa, K., Miyano, K., Yamane, T., and Sato, J. (1982) Growth of human hepatoma cells lines with differentiated functions in chemically defined medium. *Cancer Res.* **42,** 3858–3863.
25. Koutsoudakis, G., Kaul, A., Steinmann, E., Kallis, S., Lohmann, V., Pietschmann, T., et al. (2006) Characterization of the early steps of hepatitis C virus infection by using luciferase reporter viruses. *J. Virol.* **80,** 5308–5320.
26. Morikawa, K., Zhao, Z., Date, T., Miyamoto, M., Murayama, A., Akazawa, D., et al. (2007) The roles of CD81 and glycosaminoglycans in the adsorption and uptake of infectious HCV particles. *J. Med. Virol.* in press.
27. Kapadia, S. B., Barth, H., Baumert, T., McKeating, J. A., and Chisari, F. V. (2007) Initiation of hepatitis C virus infection is dependent on cholesterol and cooperativity between CD81 and scavenger receptor B type I. *J. Virol.* **81,** 374–383.
28. Grove, J., Huby, T., Stamataki, Z., Vanwolleghem, T., Meuleman, P., Farquhar, M., et al. (2007) Scavenger receptor BI and BII expression levels modulate Hepatitis C virus infectivity. *J Virol.* [Epub ahead of print].
29. Blanchard, E., Belouzard, S., Goueslain, L., Wakita, T., Dubuisson, J., Wychowski, C., et al. (2006) Hepatitis C virus entry depends on clathrin-mediated endocytosis. *J Virol.* **80,** 6964–6972.
30. Evans, M. J., von Hahn, T., Tscherne, D. M., Syder, A. J., Panis, M., Wolk, B., (2007) Claudin-1 is a hepatitis C virus co-receptor required for a late step in entry. *Nature* [Epub ahead of print].
31. Kanda, T., Basu, A., Steele, R., Wakita, T., Ryerse, JS., Ray, R., et al. (2006) Generation of infectious hepatitis C virus in immortalized human hepatocytes. *J. Virol.* **80,** 4633–4639.
32. Wagoner, J., Austin, M., Green, J., Imaizumi, T., Casola, A., Brasier, A., et al. Regulation of CXCL-8 (interleukin 8) induction by dsRNA signaling pathways during hepatitis C virus infection. *J. Virol.* **81,** 309–318.
33. Larrea, E., Riezu-Boj, J. I., Gil-Guerrero, L., Casares, N., Aldabe, R., Sarobe, P., et al. (2007) Upregulation of indoleamine 2,3 dioxygenase in hepatitis C virus infection. *J. Virol.* [Epub ahead of print].
34. Francesco, R. D., and Migliaccio, G. (2005) Challenges and successes in developing new therapies for hepatitis C. *Nature* 436, 953–960.
35. Cai, Z., Zhang, C., Chang, K-Y., Jiang, J., Ahn, B-C., Wakita, T., et al. (2005) Robust production of infectious hepatitis C virus (HCV) from stably HCV cDNA-transfected human hepatoma cells. *J. Virol.* **79,** 13963–13973.
36. Kato, T., Matsumura, T., Heller, T., Saito, S., Sapp, R. K., Murthy, K., et al. (2007) Production of infectious hepatitis C virus of various genotypes in cell culture. *J. Virol.* [Epub ahead of print].
37. Rouillé, Y., Helle, F., Delgrange, D., Roingeard, P., Voisset, C., Blanchard, E., et al. (2006) Subcellular localization of hepatitis C virus structural proteins in a cell culture system that efficiently replicates the virus. *J. Virol.* **80,** 2832–2841.
38. Shirakura, M., Murakami, K., Ichimura, T., Suzuki, R., Shimoji, T., Fukuda, K., et al. (2007) The E6AP ubiquitin ligase mediates ubiquitylation and degradation of hepatitis C virus core protein. *J. Virol.* **81,** 1174–1185.
39. Houghton, M. and Abrignani, S. (2005) Prospects for a vaccine against the hepatitis C virus. *Nature* 436, 961–966.
40. Meunier, J. C., Engle, R. E., Faulk, K., Zhao, M., Bartosch, B., Alter, H., et al. (2005) Evidence for cross-genotype neutralization of hepatitis C virus pseudo-particles and enhancement of infectivity by apolipoprotein C1. *Proc. Natl. Acad. Sci. USA* **102,** 4560–4565.
41. Yi, M., Villanueva, R. A., Thomas, D. L., Wakita, T., and Lemon, S. M. (2006) Production of infectious genotype 1a hepatitis C virus (Hutchinson strain) in cultured human hepatoma cells. *Proc. Natl. Acad. Sci. USA* **103,** 2310–2315.
42. van den Hoff, M. J., Moorman, A. F., and Lamers, W. H. (1992) Electroporation in "intracellular" buffer increases cell survival. *Nucleic Acids Res.* **20,** 2902.
43. Kato, T., Date, T., Murayama, A., Morikawa, K., Akazawa, D., and Wakita, T. (2006) Cell culture and infection system for hepatitis C virus. *Nature Protocols* **1,** 2334–2339.
44. Reed, L. J. and Muench, H. A. (1938) Simple method of estimating fifty per cent endpoints. *Am. J. Hyg.* 27493–27497.

ARTICLE IN PRESS

Biochemical and Biophysical Research Communications xxx (2008) xxx–xxx

Contents lists available at ScienceDirect

Biochemical and Biophysical Research Communications

journal homepage: www.elsevier.com/locate/ybbrc

Characterization of infectious hepatitis C virus from liver-derived cell lines

Daisuke Akazawa [a,b], Tomoko Date [b], Kenichi Morikawa [b], Asako Murayama [b], Noriaki Omi [a,b], Hitoshi Takahashi [a,b], Noriko Nakamura [a], Koji Ishii [b], Tetsuro Suzuki [b], Masashi Mizokami [c], Hidenori Mochizuki [a], Takaji Wakita [b,*]

[a] Pharmaceutical Research Laboratories, Toray Industries, Inc., Kanagawa, Japan
[b] Department of Virology II, National Institute of Infectious Diseases, 1-23-1 Toyama, Shinjuku-ku, Tokyo 162-8640, Japan
[c] Department of Clinical Molecular Informative Medicine, Nagoya City University Graduate School of Medical Sciences, Nagoya, Japan

ARTICLE INFO

Article history:
Received 20 September 2008
Available online xxxx

Keywords:
Cell culture
Hepatitis C virus
Infectivity
Particle
Replicon

ABSTRACT

The efficient production of infectious HCV from the JFH-1 strain is restricted to the Huh7 cell line and its derivatives. However, the factors involved in this restriction are unknown. In this study, we examined the production of infectious HCV from other liver-derived cell lines, and characterized the produced viruses. Clones of the Huh7, HepG2, and IMY-N9, harboring the JFH-1 full-genomic replicon, were obtained. The supernatant of each cell clone exhibited infectivity for naïve Huh7. Each infectious supernatant was then characterized by sucrose density gradient. For all of the cell lines, the main peak of the HCV-core protein and RNA exhibited at approximately 1.15 g/mL of buoyant density. However, the supernatant from the IMY-N9 differed from that of Huh7 in the ratio of core:RNA at 1.15 g/mL and significant peaks were also observed at lower density. The virus particles produced from the different cell lines may have different characteristics.

Hepatitis C virus (HCV) is an enveloped virus that belongs to the *Hepacivirus* genus of the *Flaviviridae* family. HCV is a human pathogen and HCV infection is a major cause of chronic hepatitis, liver cirrhosis and hepatic carcinoma. The main therapy for HCV is treatment with pegylated-interferon and rivabirin. However, these agents show little effect for patients that have a high titer of HCV-RNA, genotype 1. Thus, it is necessary to develop new, more effective therapies and preventive treatments to counteract HCV infection. It was discovered that a genotype 2a strain of HCV, JFH-1, can efficiently replicate in the Huh7 cell line [1], and an *in vitro* culture model of infectious HCV has also been successfully developed using the JFH-1 genome [2–4]. Recently, it has become possible to produce various chimeric HCV by replacement of the JFH-1 structural protein region with that of other strains. The HCV particles produced from such chimera are expected to lead to the development of a HCV vaccine, and new anti-HCV pharmaceuticals.

The infectious HCV-derived JFH-1 genome was developed using the human hepatoma Huh7 cell line [5]. Although the sub-genomic replicon RNA of JFH-1 can autonomously replicate, not only in Huh7 cells, but in other human liver [6], non-hepatic [7], and mouse [8] cells, infectious HCV production has been restricted to Huh7-derived cells. In this study, we undertook a comparative study of infectious HCV particles produced from different cell lines including Huh7. Infectious HCV particles were successfully produced into the culture media and characterized.

Materials and methods

Cell culture. Huh7, Huh7.5.1 ([3], a generous gift from Dr. Francis V. Chisari), HepG2, and IMY-N9 cells were cultured at 37 °C in 5% CO_2. The HepG2 cells were cultured in modified Eagle's medium containing 10% fetal bovine serum. All of the other cells were cultured in Dulbecco's modified Eagle's medium containing 10% fetal bovine serum, as described previously [6].

Plasmids. The pFGR-JFH1 and pFGR-JFH1/deltaE12 plasmids, encoding the full-genomic replicon, and envelope-deleted replicons, respectively, were generated as previously described [9].

RNA synthesis. RNA synthesis was performed as described previously [2]. Briefly, the pFGR-JFH1 plasmid was digested with XbaI and then treated with Mung Bean nuclease (New England Biolabs, Beverly, MA). The digested plasmid DNA fragment was then purified and used as a template for RNA synthesis. HCV-RNA was synthesized *in vitro* using a MEGAscript™ T7 kit (Ambion, Austin, TX). The synthesized RNA was treated with DNaseI, followed by acid phenol extraction to remove any remaining template DNA.

Establishment of replicon cells. Cell lines harboring FGR-JFH1 replicons were produced as described previously [9]. Briefly, trypsinized cells were washed with Opti-MEM I™ reduced-serum medium (Invitrogen, Carlsbad, CA) and resuspended at 7.5×10^6 cells/mL with Cytomix buffer [1]. RNA (10 μg), synthesized from pFGR-JFH1, was mixed with 400 μL of cell suspension and transferred to an electroporation cuvette (Precision Universal Cuvettes, Thermo Hybrid, Middlesex, UK). The cells were then pulsed at 260 V and 950 μF with the Gene Pulser II™ apparatus (Bio-Rad,

* Corresponding author. Fax: +81 3 5285 1161.
E-mail address: wakita@nih.go.jp (T. Wakita).

0006-291X/$ - see front matter © 2008 Elsevier Inc. All rights reserved.
doi:10.1016/j.bbrc.2008.10.063

Please cite this article in press as: D. Akazawa et al., Characterization of infectious hepatitis C virus from liver-derived cell lines..., Biochem. Biophys. Res. Commun. (2008), doi:10.1016/j.bbrc.2008.10.063

Hercules, CA). Transfected cells were immediately transferred to 10-cm culture dishes, each containing 8 mL of culture medium. G418 (0.8–1.0 mg/mL) (Nacalai Tesque, Kyoto, Japan) was added to the culture medium at 16–24 h after transfection. Culture medium, supplemented with G418, was replaced twice per week. Three weeks after transfection, sparsely grown G418-resistant colonies were independently isolated using a cloning cylinder (Asahi Techno Glass Co., Tokyo, Japan), and were expanded.

Preparation of supernatants from FGR-JFH1 replicon cells. Culture media was collected from Huh7, IMY-N9, and HepG2 cell lines harboring the FGR-JFH1 replicon and was passed through a 0.45-μm filter. Filtrated culture media was then pooled and concentrated 50-fold using Amicon Ultra-15 (100,000 Molecular weight cut off; Millipore, Bedford, MA), and stored at −80 °C until use.

Assay of infection of naïve Huh7 cells. Infection of naïve Huh7 cells were assayed by immunofluorescence and colony formation assays. For the immunofluorescence assay naïve Huh7.5.1 cells were seeded at 1×10^4 cells/well in an 8-well chamber slide (Becton Dickinson, Franklin Lakes, NJ), cultured overnight and then inoculated with diluted culture media containing infectious HCV particles (1×10^6 HCV-RNA copies). At 72 h after inoculation, the cells were fixed in acetone/methanol (1:1) for 10 min at −20 °C, and the infected foci were visualized by immunofluorescence as follows.

An anti-core HCV protein monoclonal antibody 2H9 [2] was added to the cells at 50 μg/mL in BlockAce (Dainippon Sumitomo Pharma, Osaka, Japan). After incubation for 1 h at room temperature, the cells were washed and incubated with a 1:400 dilution of AlexaFluor 488-conjugated anti-mouse IgG (Molecular Probes, Eugene, OR) diluted in BlockAce. The cells were then washed, treated with DAPI solution (Sigma, Saint Louis, MO) at 0.1 μg/mL and examined by Biozero fluorescence microscopy (Keyence, Osaka, Japan).

Colony formation assays were performed as described previously [9]. Briefly, naïve Huh7 cells were inoculated with culture supernatants from replicon-expressing cell lines for 2 h, and then cultured with complete medium. Inoculated cells were cultured for 3 weeks in medium supplemented with G418 (0.3 mg/mL). Cell survival was assessed by staining with crystal violet.

Titration of infectivity. The infectivity titer of the culture supernatants was determined on Huh7.5.1 cells by end point dilution and immunofluorescence as described above. Briefly, each sample was serially diluted 10-fold in DMEM-10% FBS and 100 μL was used to inoculate Huh7.5.1 cells. Infection was examined 72 h post-inoculation by immunofluorescence using a mouse monoclonal anti-core antibody and secondary anti-mouse IgG-Alexa 488 conjugated antibodies. Infectious foci were counted and the titer was calculated and expressed as focus forming units per mL (FFU/mL).

Sucrose density gradient analysis. Concentrated cell supernatants were layered on top of a preformed continuous 10–60% sucrose gradient in TNE buffer containing 10 mM Tris, pH7.5, 150 mM NaCl, and 0.1 mM EDTA. Gradients were centrifuged in an SW41 rotor (Beckman Coulter, Fullerton, CA) at 35,000 rpm for 16 h at 4 °C, and fractions (400 μL each) were collected from the bottom of the tube. The density of each fraction was estimated by weighing a 100 μL drop from each fraction following a gradient run.

Quantification of HCV-core protein and RNA. The level of the HCV-core protein in culture supernatants or sucrose density gradient fractions, was assayed using an immunoassay as described elsewhere [10]. Viral RNA was isolated from harvested culture media, or sucrose density gradient fractions, using the QiaAmp Viral RNA Extraction kit (Qiagen, Tokyo, Japan). The copy number of HCV RNA was determined by real-time detection reverse transcription-polymerase chain reaction (RTD-PCR), using an ABI Prism 7500fast sequence detector system (Applied Biosystems, Tokyo, Japan) [11].

Results

Production of infectious HCV from human liver-derived cell lines

We first determined if it was possible to produce infectious HCV from cell lines other than Huh7. We selected the HepG2 and IMY-N9 cell lines to establish human liver-derived cell lines that enable replication of the JFH-1 genome [6]. Since full-genomic JFH-1 did not transiently replicate in these cells (data not shown), we established FGR-JFH1 replicon cells that stably replicate the JFH-1 genome. In the culture media obtained from these full-genomic replicon cells, HCV-RNA titers were detected by RTD-PCR. The titer of HCV-RNA was highest in the supernatant from an IMY-N9 cell clone and lowest from a HepG2 cell clone (Table 1). When naïve Huh7.5.1 cells were inoculated with culture supernatants from the replicon cells, infected cells could be detected by immunofluorescence using an anti-HCV-core protein antibody (Fig. 1A). These data suggested that HepG2 and IMY-N9 cells are able to produce infectious HCV.

We then compared the specific infectivity of the replicon containing culture supernatants from the different cells. Specific infectivity was calculated by dividing the infectious titer, calculated by immunofluorescence of infectious foci, of the culture media by the titer obtained for HCV-RNA. Using these calculations the culture media from Huh7 and HepG2 cells showed almost the same specific infectivity whereas that from IMY-N9 cell was relatively higher (Table 1). Thus the infectious HCV in the culture media might differ according to the cell line from which it was obtained.

To clarify the differences observed in specific infectivity, we next examined the ability of the various cellular supernatants to induce colony formation. For this assay naïve Huh7 cells were inoculated with culture media of the same HCV-RNA titer as that of the FGR-JFH1 virus and were cultured in G418-containing medium. Cell survival was assayed by staining with crystal violet, and the number of colonies formed was counted. Consistent with the specific infectivity results, the supernatant of the IMY-N9 replicon cell showed higher colony formation compared with that of Huh7 and HepG2 replicon cells (Fig. 1B and C). Thus IMY-N9 cells produce infectious HCV with a relatively higher infectivity than the other cell lines suggesting that the supernatant derived from the different replicon producing cells may differ.

Characterization of the FGR-JFH1 virus from different liver-derived cells

To further characterize potential differences between the viruses produced by the different cell lines we next characterized the FGR-JFH1 virus in the media of the different cell lines by sucrose density gradient analysis. Concentrated cell supernatants were layered on top of a preformed continuous 10–60% sucrose gradient and centrifuged. Twenty-four fractions were collected and the HCV-core protein and RNA was assayed in each fraction. The peak fraction of the HCV-core protein and that of the RNA coincided at a density of 1.15 g/mL in all supernatants. However, the supernatant of the IMY-N9 cells showed different profiles for both the HCV-core protein and RNA compared to those of Huh7. Thus the IMY-N9 cells had a different ratio of

Table 1
Infectivity of the supernatant of replicon cell lines.

Producing cell	HCV-RNA (copies/mL)	Infectious titer (FFU/mL)	Specific infectivity (FFU/RNA copy)
Huh7	$1.36 \pm 0.02 \times 10^8$	$1.30 \pm 0.32 \times 10^4$	9.56×10^{-5}
IMY-N9	$2.80 \pm 0.04 \times 10^8$	$3.75 \pm 0.38 \times 10^4$	1.34×10^{-4}
HepG2	$8.80 \pm 0.75 \times 10^7$	$7.70 \pm 1.41 \times 10^3$	7.96×10^{-5}

Please cite this article in press as: D. Akazawa et al., Characterization of infectious hepatitis C virus from liver-derived cell lines..., Biochem. Biophys. Res. Commun. (2008), doi:10.1016/j.bbrc.2008.10.063

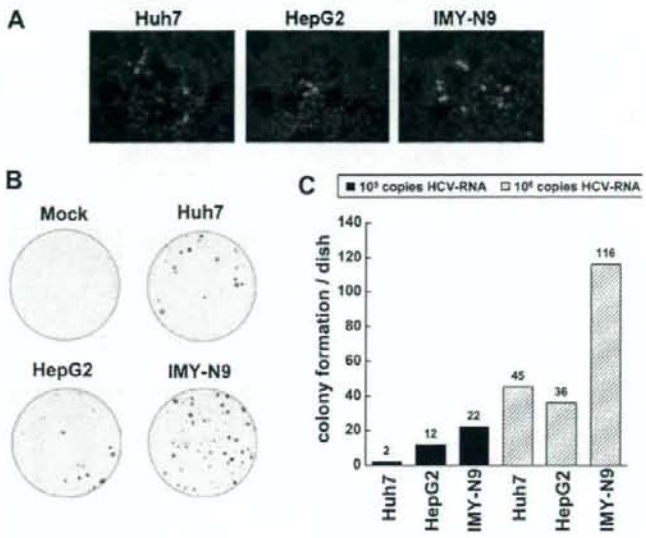

Fig. 1. Naïve Huh7 cell infection assay of JFH-1 full-genomic replicon cell culture supernatants. (A) JFH-1 full-genomic replicon (FGR-JFH1) cells were established in Huh7, HepG2, and IMY-N9 cell lines. Supernatants derived from Huh7 (*left*), HepG2 (*middle*), and IMY-N9 (*right*) cells (1×10^6 HCV-RNA copies) were inoculated into naïve Huh7.5.1 cells (1×10^4) for 48 h, and infected cells were then detected by immunofluorescence using an anti-core antibody (clone 2H9) (green). (B) Naïve Huh7 cells (5×10^5) were inoculated with mock, Huh7, HepG2, and IMY-N9-derived supernatants (10^6 HCV-RNA copies per 10-cm dish) of FGR-JFH1 cells for 2 h. Inoculated cells were cultured for 3 weeks in complete medium supplemented with G418 (0.3 mg/mL), and G418-resistant cells were stained using crystal violet. (C) The number of G418-resistant colonies obtained in (B) was calculated when 10^5 or 10^6 copies of HCV-RNA were tested. Mean values of colony number were indicated in duplicate experiment. (For interpretation of the references to color in this figure legend, the reader is referred to the web version of this article.)

HCV-core protein and RNA at a density of 1.15 g/mL (RNA/Core ratio; Huh7: 511, IMY-N9: 133 copies/fmol) and also showed a secondary peak at lower density (approximately 1.05 g/mL). For all supernatants the peak of infectivity exhibited at a density of 1.10 g/mL that was slightly lower than that of the HCV-core protein and RNA peaks. Furthermore infectivity was barely detectable in the lower density fractions (Fig. 2) suggesting that the HCV-core protein and RNA that was detected at lower density was irrelevant for infectivity of the different supernatants.

We considered the possibility that the core protein and RNA in the lighter fractions may be due to cellular debris containing a replication complex. To determine if this might be the case we therefore analyzed the supernatants from Huh7 and IMY-N9 envelope-deleted replicon cells (FGR-JFH1/deltaE12). The HCV-core protein and RNA were detected in the supernatants of these cells although the titers were very low. These supernatants were not infective for naïve Huh7 cells (data not shown). Furthermore, analysis of the concentrated supernatants of these cell lines by sucrose density gradient analysis detected both the HCV-core protein and RNA, and the major peaks of HCV-RNA were detected in the lower density (approximately 1.10 g/mL) fractions (Fig. 3). However, the profiles of HCV-core protein and RNA did not coincide for either cell line.

Discussion

Infectious HCV can be produced in cell culture by using the JFH-1 genome. This system permits investigation of various aspects of the HCV life cycle such as the steps of entry into cells, replication, and secretion. Infectious HCV derived from JFH-1 is robustly produced in Huh7 cell lines [2,3], and the infectious particles have been characterized. However the difficulty in robustly producing infectious HCV from other cell lines prevents a comparative study of HCV production among different cell lines. In this study, we compared infectious HCV production in Huh7 with that of other cell lines, and characterized the viruses produced.

First, we established Huh7, IMY-N9, and HepG2 FGR-JFH1 replicon cells. These cell lines were able to replicate the JFH-1 subgenomic replicon [6]. The HCV-core protein and RNA were detected in all of the supernatants and all of these supernatants showed infectivity for naïve Huh7. Infectivity was evaluated by transient infection and colony formation assays. These assays indicated that the infectious supernatant from IMY-N9 cell had higher infectivity than the other cell lines for naïve Huh7 cells.

Next, we characterized each supernatant by sucrose density gradient analysis, which revealed both similarities and differences among the infectious supernatants. All samples showed typical peaks at 1.15 g/mL buoyant density for HCV-core protein and RNA, and infectious fractions showed an almost identical buoyant density of 1.10 g/mL. However, the supernatant from the IMY-N9 cells showed a difference in the core/RNA ratio at a density of 1.15 g/mL and higher secondary peak of HCV-core protein and RNA at a lower density (approximately 1.05 g/mL). Since the fractions at lower density did not correlate with infectivity, it is believed that the component at lower density does not contain infectious HCV particles but rather cellular debris that contains HCV proteins, RNA, and lipids [12]. HCV can associate with lipoprotein [13,14], and is secreted with VLDL [15]. Thus, the observed differences in the HCV-producing cells may derive from differences in lipoprotein synthesis. However, it is also possible that the components migrating at lower density contain virus particles. The deletion mutant of FGR-JFH1 (FGR-JFH1/deltaE12) did replicate in Huh7 and IMY-N9 cells, and these replicon cells secreted the HCV-core protein into the culture media, although at low levels. HCV-RNA was also detected in the same culture

Please cite this article in press as: D. Akazawa et al., Characterization of infectious hepatitis C virus from liver-derived cell lines..., Biochem. Biophys. Res. Commun. (2008), doi:10.1016/j.bbrc.2008.10.063

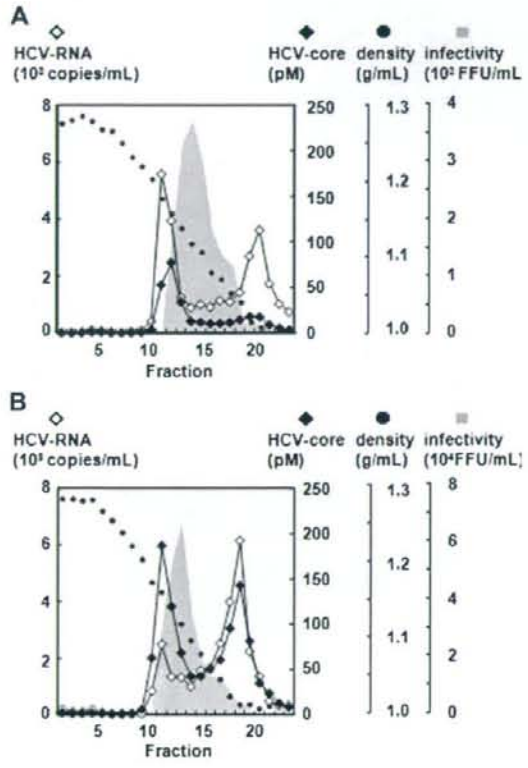

Fig. 2. Density gradient analysis of infectious HCV derived from Huh7 and IMY-N9 cells. Concentrated supernatants of Huh7 cells (A) and IMY-N9 cells (B) were layered on top of a preformed continuous 10–60% sucrose gradient in TNE buffer. The gradients were centrifuged in a SW41 rotor at 35,000 rpm for 16 h at 4 °C, and fractions (400 μL each) were collected from the bottom of the tube. The buoyant density (closed circles), HCV-core protein (closed diamonds), HCV-RNA (open diamonds) and infectivity for naïve Huh7.5.1 cells (shown in gray) was detected in each fraction as described in Materials and methods.

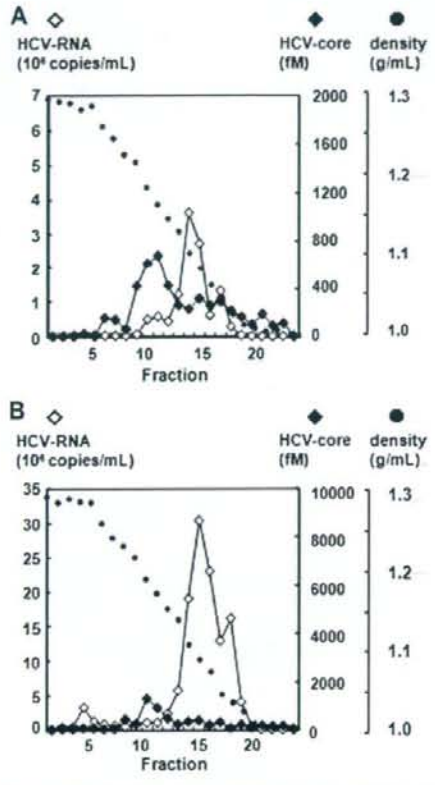

Fig. 3. Density gradient analysis of supernatants derived from Huh7 and IMY-N9 cells transfected with FGR-JFH1/deltaE12 RNA. Concentrated supernatants from Huh7 (A) and IMY-N9 (B) cells were analyzed by sucrose density gradient as described in the legend to Fig. 2. The buoyant density (closed circles), HCV-core protein (closed diamonds) and HCV-RNA (open diamonds) was analyzed in each fraction.

medium, and the profile of this HCV-RNA differed from that of the HCV-core protein in sucrose density gradient analysis. Thus, the peak fractions containing the HCV-core protein and RNA from the supernatant of FGR-JFH1/deltaE12 cells were different from the peak fractions from that of FGR-JFH1 cells. Therefore it is possible that all of the peaks of HCV-core protein and RNA observed in the supernatant of FGR-JFH1 replicon cells may correlate to virus particles with different densities. However, the reason why they centrifuge at different densities is unclear. Interestingly, the supernatants from cells transfected with envelope-deleted replicon RNA exhibit non-identical HCV-core protein and RNA profiles on a sucrose density gradient. Envelope-deleted replicon RNA may have a decreased ability to form nucleocapsids although a detailed examination is necessary to establish this point.

We previously developed a method for infectious HCV production using the FGR-JFH1 [9], and have now succeeded in producing infectious HCV in the supernatant of cultured liver-derived cell lines harboring FGR-JFH1 RNA. Infectious HCV particles are useful for vaccine production and are considered good antigens for the generation of useful antibodies. Selection of an appropriate cell line is important for the production of HCV particles for vaccine development. The technique used in this study seemed to be appropriate for producing infectious HCV in various cell lines [8].

A second advantage of using HepG2 and IMY-N9 cells for the production of virus particles is that these parental cell lines, unlike the Huh7 cell line, do not express the CD81 molecule on the cell surface, however, the expression on cell clones used in this study was not confirmed. This means that the FGR-JFH1 replicon of these cell lines may have a single cycle of HCV production, encompassing replication, assembly, budding and secretion, and do not show HCV permissiveness. These cells should therefore be useful for the discovery of drugs targeted against HCV assembly and secretion.

Acknowledgments

This work was partially supported by a grant-in-aid for Scientific Research from the Japan Society for the Promotion of Science and from the Ministry of Health, Labor, and Welfare of Japan by the Research on Health Sciences Focusing on Drug Innovation from the Japan Health Sciences Foundation. Huh7 and Huh7.5.1 was a kind gift from Dr. Francis V. Chisari.

References

[1] T. Kato, T. Date, M. Miyamoto, A. Furusaka, K. Tokushige, M. Mizokami, T. Wakita, Efficient replication of the genotype 2a hepatitis C virus subgenomic replicon, Gastroenterology 125 (2003) 1808–1817.

Please cite this article in press as: D. Akazawa et al., Characterization of infectious hepatitis C virus from liver-derived cell lines..., Biochem. Biophys. Res. Commun. (2008), doi:10.1016/j.bbrc.2008.10.063

[2] T. Wakita, T. Pietschmann, T. Kato, T. Date, M. Miyamoto, Z. Zhao, K. Murthy, A. Habermann, H.G. Krausslich, M. Mizokami, R. Bartenschlager, T.J. Liang, Production of infectious hepatitis C virus in tissue culture from a cloned viral genome, Nat. Med. 11 (2005) 791–796.
[3] J. Zhong, P. Gastaminza, G. Cheng, S. Kapadia, T. Kato, D.R. Burton, S.F. Wieland, S.L. Uprichard, T. Wakita, F.V. Chisari, Robust hepatitis C virus infection in vitro, Proc. Natl. Acad. Sci. USA 102 (2005) 9294–9299.
[4] B.D. Lindenbach, M.J. Evans, A.J. Syder, B. Wolk, T.L. Tellinghuisen, C.C. Liu, T. Maruyama, R.O. Hynes, D.R. Burton, J.A. McKeating, C.M. Rice, Complete replication of hepatitis C virus in cell culture, Science 309 (2005) 623–626.
[5] H. Nakabayashi, K. Taketa, K. Miyano, T. Yamane, J. Sato, Growth of human hepatoma cells lines with differentiated functions in chemically defined medium, Cancer Res. 42 (1982) 3858–3863.
[6] T. Date, T. Kato, M. Miyamoto, Z. Zhao, K. Yasui, M. Mizokami, T. Wakita, Genotype 2a hepatitis C virus subgenomic replicon can replicate in HepG2 and IMY-N9 cells, J. Biol. Chem. 279 (2004) 22371–22376.
[7] T. Kato, T. Date, M. Miyamoto, Z. Zhao, M. Mizokami, T. Wakita, Nonhepatic cell lines HeLa and 293 support efficient replication of the hepatitis C virus genotype 2a subgenomic replicon, J. Virol. 79 (2005) 592–596.
[8] S.L. Uprichard, J. Chung, F.V. Chisari, T. Wakita, Replication of a hepatitis C virus replicon clone in mouse cells, Virol. J. 3 (2006) 89.
[9] T. Date, M. Miyamoto, T. Kato, K. Morikawa, A. Murayama, D. Akazawa, J. Tanabe, S. Sone, M. Mizokami, T. Wakita, An infectious and selectable full-length replicon system with hepatitis C virus JFH-1 strain, Hepatol. Res. 37 (2007) 433–443.
[10] K. Aoyagi, C. Ohue, K. Iida, T. Kimura, E. Tanaka, K. Kiyosawa, S. Yagi, Development of a simple and highly sensitive enzyme immunoassay for hepatitis C virus core antigen, J. Clin. Microbiol. 37 (1999) 1802–1808.
[11] T. Takeuchi, A. Katsume, T. Tanaka, A. Abe, K. Inoue, K. Tsukiyama-Kohara, R. Kawaguchi, S. Tanaka, M. Kohara, Real-time detection system for quantification of hepatitis C virus genome, Gastroenterology 116 (1999) 636–642.
[12] T. Pietschmann, V. Lohmann, A. Kaul, N. Krieger, G. Rinck, G. Rutter, D. Strand, R. Bartenschlager, Persistent and transient replication of full-length hepatitis C virus genomes in cell culture, J. Virol. 76 (2002) 4008–4021.
[13] M. Monazahian, S. Kippenberger, A. Muller, H. Seitz, I. Bohme, S. Grethe, R. Thomssen, Binding of human lipoproteins (low, very low, high density lipoproteins) to recombinant envelope proteins of hepatitis C virus, Med. Microbiol. Immunol. 188 (2000) 177–184.
[14] R. Thomssen, S. Bonk, C. Propfe, K.H. Heermann, H.G. Kochel, A. Uy, Association of hepatitis C virus in human sera with beta-lipoprotein, Med. Microbiol. Immunol. 181 (1992) 293–300.
[15] S.U. Nielsen, M.F. Bassendine, A.D. Burt, C. Martin, W. Pumeechockchai, G.L. Toms, Association between hepatitis C virus and very-low-density lipoprotein (VLDL)/LDL analyzed in iodixanol density gradients, J. Virol. 80 (2006) 2418–2428.

Please cite this article in press as: D. Akazawa et al., Characterization of infectious hepatitis C virus from liver-derived cell lines..., Biochem. Biophys. Res. Commun. (2008), doi:10.1016/j.bbrc.2008.10.063

Hepatitis C Virus Infection Sensitizes Human Hepatocytes to TRAIL-Induced Apoptosis in a Caspase 9-Dependent Manner[1]

Lin Lan,[2*†] Sebastian Gorke,[2*‡] Sibylle J. Rau,[*‡] Mirjam B. Zeisel,[§¶] Eberhard Hildt,[*‖] Kiyoshi Himmelsbach,[*‡‖] Monica Carvajal-Yepes,[*‡‖] Roman Huber,[*] Takaji Wakita,[#] Annette Schmitt-Graeff,[**] Cathy Royer,[§¶] Hubert E. Blum,[*] Richard Fischer,[3,4*] and Thomas F. Baumert[3§¶††]

Apoptosis of infected cells represents a key host defense mechanism against viral infections. The impact of apoptosis on the elimination of hepatitis C virus (HCV)-infected cells is poorly understood. The TRAIL has been implicated in the death of liver cells in hepatitis-infected but not in normal liver cells. To determine the impact of TRAIL on apoptosis of virus-infected host cells, we studied TRAIL-induced apoptosis in a tissue culture model system for HCV infection. We demonstrated that HCV infection sensitizes primary human hepatocytes and Huh7.5 hepatoma cells to TRAIL induced apoptosis in a dose- and time-dependent manner. Mapping studies identified the HCV nonstructural proteins as key mediators of sensitization to TRAIL. Using a panel of inhibitors targeting different apoptosis pathways, we demonstrate that sensitization to TRAIL is caspase-9 dependent and mediated in part via the mitochondrial pathway. Sensitization of hepatocytes to TRAIL-induced apoptosis by HCV infection represents a novel antiviral host defense mechanism that may have important implications for the pathogenesis of HCV infection and may contribute to the elimination of virus-infected hepatocytes. ***The Journal of Immunology*****, 2008, 181: 4926–4935.**

Hepatitis C virus (HCV)[5] infection is a leading cause of liver cirrhosis and hepatocellular carcinoma (1). HCV belongs to the *Flaviviridae* family and has an enveloped, positive-stranded RNA genome of 9.6 kb length containing one open reading frame translated into a single polyprotein. A highly conserved, untranslated region at the 5′ site serves as an internal ribosomal entry site which directs cap-independent translation. Posttranslational cleavage of the polyprotein yields in structural and nonstructual proteins including core, E1, E2, p7, NS2, NS3, NS4A, NS4B, NS5A, and NS5B (2, 3).

Histopathological studies demonstrated that enhanced hepatocyte apoptosis is a common feature in the HCV-infected liver (4, 5). The close physical proximity of apoptotic hepatocytes and infiltrating lymphocytes seen in HCV infection suggests that apoptosis is initiated by an interaction between effector cells of the host immune system and hepatoyctes (4). Effector cells of the innate and acquired immune system are able to kill target cells through ligands of the death receptor family. In contrast to TNF-α and CD95/Fas, TRAIL induces apoptosis only in infected or transformed tumor cells (6). In line with these observations, TRAIL does not induce apoptosis in noninfected healthy hepatocytes in vivo (5, 7). For all three death ligands an up-regulation of expression has been described in chronic HCV infection (4, 5, 8). TRAIL binding induces the formation of a death-inducing signaling complex, resulting in the activation of caspase-8. Active caspase-8 can trigger two signaling pathways, the first involving direct activation of caspase-3, the second involving cleavage of Bid, followed by mitochondria-dependent activation of caspase-9 via cytochrome C release and Apaf-1 activation (9). Hepatocytes most likely represent so-called type-II cells, for which external activation of the death signaling pathway often is insufficient to induce apoptosis and requires in addition amplification by the mitochondrial pathway (intrinsic apoptosis pathway). The latter is affected by oxidative stress, DNA damage, and viral proteins (10, 11). Mitochondria-dependent apoptosis is amplified by proapoptotic Bax, Bad,

*Department of Medicine II, University of Freiburg, Germany; †Institute of Infectious Diseases, Southwestern Hospital, Third Military Medical University, Chongqing, China; ‡Faculty of Biology, University of Freiburg, Freiburg, Germany; §Institut National de la Santé et de la Recherche Médicale, U748, Strasbourg, France; ¶Université Louis Pasteur, Strasbourg, France; ‖Institute for Infection Medicine, Molecular Medical Virology, University of Kiel, Kiel, Germany; #Department of Virology II, National Institute of Infectious Diseases, Tokyo, Japan; **Institute of Pathology, University of Freiburg, Freiburg, Germany; and ††Service d'Hépatogastroentérologie, Hôpitaux Universitaires de Strasbourg, Strasbourg, France

Received for publication December 21, 2007. Accepted for publication July 23, 2008.

The costs of publication of this article were defrayed in part by the payment of page charges. This article must therefore be hereby marked *advertisement* in accordance with 18 U.S.C. Section 1734 solely to indicate this fact.

[1] This study was supported by the Fritz Thyssen Stiftung (to R.F.), Germany, the Faculty of Medicine, University of Freiburg, Germany (to R.F. and A.S.-G.), and by grants of Institut National de la Santé et de la Recherche Médicale, France, the European Union (LSHM-CT-2004–503359 "VIRGIL"; to T.F.B.), Belgium, the chair of excellence program of the Agence Nationale de la Recherche (ANR-05-CEXC-008; to T.F.B.), France, the Agence Nationale de la Recherche sur le SIDA et les Hépatites Virales (ANRS 06221; to T.F.B.), France, the Deutsche Forschungsgemeinschaft (Ba1417/11–2; to T.F.B.), Germany, France and the Else Kröner-Fresenius Foundation, Bad Homburg, Germany (P17/07//A83/06; T. F. B.). M.B.Z. was supported by the Inserm *Poste Vert* program in the framework of Institut National de la Santé et de la Recherche Médicale European Associated Laboratory Freiburg-Strasbourg. T.W. is supported by a grant-in-aid for Scientific Research from the Japan Society for the Promotion of Science, from the Ministry of Health, Labour and Welfare of Japan and from the Ministry of Education, Culture, Sports, Science and Technology, and by the Research on Health Sciences Focusing on Drug Innovation from the Japan Health Sciences Foundation.

[2] L.L. and S.G. contributed equally to this study.

[3] R.F. and T.F.B. contributed equally to this study.

[4] Address correspondence and reprint requests to Dr. Richard Fischer, Department of Medicine II, University of Freiburg, Hugstetter Strasse 55, D-79106 Freiburg, Germany. E-mail address: richard.fischer.medizin@uniklinik-freiburg.de

[5] Abbreviations used in this paper: HCV, hepatitis C virus; PHH, primary human hepatocyte; MOI, multiplicity of infection; JFH1, Japanese fulminant hepatitis 1 isolate; HCVcc, cell culture-derived HCV; PARP, poly (ADP-ribose) polymerase; HBV, hepatitis B virus.

Bak, and other proteins, while Bcl-2 or Bcl-x_L act anti-apoptotic (for review see Ref.12).

The molecular mechanisms of hepatocyte apoptosis in HCV infection are poorly understood. For both HCV structural and nonstructural proteins, pro- and antiapoptotic properties have been described (13). Viral RNA has been shown to be able to induce apoptosis via activation of protein kinase R and the retinoic acid inducible gene-I-Cardif pathway (14–16). However, the significance of these interactions for productive viral infection and pathogenesis of HCV-induced liver disease remains unknown. Studies on HCV-host interactions had been hampered for a long time by the lack of an efficient tissue culture model for HCV infection. Thus, alternative model systems, such as recombinant proteins, pseudotype particles, or subgenomic replicons, had been developed for the study of defined aspects of the HCV life cycle (for review see Ref. 17). A major breakthrough for the study of HCV-host cell interaction was the recent establishment of an efficient cell culture system for HCV (18–20). This model system now allows the study of HCV-host interactions and apoptosis in the context of the complete viral life cycle in human hepatocyte-derived target cells.

To determine the impact of TRAIL on apoptosis of virus-infected host cells, we studied mechanisms of TRAIL-induced apoptosis in a tissue culture model system for HCV infection.

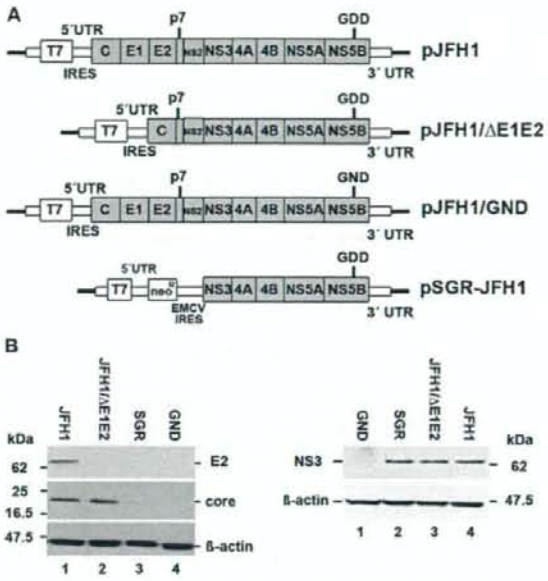

FIGURE 1. HCV constructs and viral protein expression. *A*, Constructs: HCV-pJFH1 resulting in the production of infectious viral particles, pJFH1/ΔE1E2 containing a deletion of the HCV envelope protein coding region preventing production of infectious viral particles, pJFH1/GND containing a mutation in NS5B protein preventing viral replication, and subgenomic replicon pSGR-JFH1 (lacking the coding region for HCV structural proteins and NS2, respectively). *B*, Protein expression from replication-competent constructs. Seventy-two hours following electroporation with HCV RNA transcribed from constructs depicted in *A*, cells were lysed and subjected to immunoblot analysis using Abs against HCV core, E2, NS3, and NS5A proteins as described in *Materials and Methods*.

Materials and Methods

Cells

Primary human hepatocytes (PHH) were isolated and cultured as described (21). Human hepatoma cells Huh7.5 have been described (18, 22).

Constructs

Plasmids pJFH1, pJFH1/ΔE1E2, pJFH1/GND, pSGR-JFH1, pSGR-JFH1/GND, and pFK-Jc1 have been described (19, 23, 24) and are depicted in Fig. 1.

Electroporation of HCV RNA, cell culture-derived HCV (HCVcc) production, infection of Huh7.5 cells, and PHH

Electroporation of RNA derived from plasmids pJFH1, pJFH1/ΔE1E2, pJFH1/GND, pSGR-JFH1, pSGR-JFH1/GND, and pFK-Jc1 was performed as described (19, 23, 24). Culture supernatants from HCV JFH1[6], HCV Jc1, and HCV JFH1/ΔE1E2 RNA transfected cells were harvested, concentrated and used to infect naive Huh7.5 cells (22) as well as primary human hepatocytes. Culture supernatants used to infect naive Huh7.5 cells had a $TCID_{50}$ of 10^4/ml for JFH1 and 10^5-10^6/ml for Jc1.

Immunoblot analysis of viral and cellular proteins

Cell lysis, protein determination, Western blot analysis, and densitometric analysis were performed as recently described (25). Cytosolic and mitochondrial protein fractions were obtained using a ProteoExtract Subcellular Proteome Extraction Kit according to the manufacturer's protocol (Calbiochem). Relative OD was calculated by correlation of the given protein to β-actin; maximal intensity was arbitrarily set to 100. At least three independent experiments were performed; the mean relative OD and the corresponding SEM is given. Protein loading was controlled by staining the membranes with Coomassie-blue and blotting of β-actin. Immunoblot analysis of HCV core, E2, and NS5A protein was performed using monoclonal mouse anti-core (28), anti-E2 (26), and polyclonal anti-NS5A Abs (27). mAbs directed against NS3 (ViroStat), caspase-3 (3G2, Cell Signaling Technology), caspase-8 (1C12, Cell Signaling Technology), caspase-9 (C9, Cell Signaling Technology), β-actin (Sigma-Aldrich), cleaved poly (ADP-ribose) polymerase (PARP) (Asp214, Cell Signaling Technology), TRAIL-R1, -R2, and TRAIL (R&D Systems), Bcl-2 and Bcl-x_L (Santa Cruz Biotechnology), cytochrome C (Biovision), and HRP-linked species-specific Abs (Amersham Biosciences) were used for immunoblot analysis of the respective proteins.

Induction of apoptosis by TRAIL

Naive and HCV RNA transfected Huh7.5 cells were seeded at a density of 2–4 × 10^5 cells/well in 6-well plates 72 h before apoptosis experiments. Cells were washed with PBS and incubated in cell culture medium with recombinant TRAIL that includes the extra cellular domain of human TRAIL (aa 95–281) fused at the N terminus to a His-tag and a linker peptide (SuperKillerTRAIL, Axxora). Alternatively, cells were preincubated in the presence or absence of caspase inhibitors (caspase-3 inhibitor (2-(4-Methyl-8-(morpholin-4-ylsulfonyl)-1,3-dioxo −1,3-dihydro-2H-pyrrolo [3,4-c]quinolin-2-yl)-ethyl-acetate), caspase-8 inhibitor: Z-IETD-FMK, caspase-10 inhibitor: Z-AEVD-FMK, caspase-9 inhibitor: Z-LEHDFMK; all from R&D Systems), Bcl-2/Bcl-x_L inhibitors (dimethoxy-dihydro-dibenzodiazocine dioxide and dimethoxy-dinitrosobenzyl; Calbiochem), or Bcl-x_L mimetic peptide (Calbiochem) containing the human conserved N-terminal homology domain of Bcl-x_L (aa 4–23), linked to a carrier peptide. Subsequently, cells were washed with PBS and harvested in lysis buffer for Western blot analysis or fixed for immunofluorescence staining.

Immunofluorescence staining of viral proteins in infected host cells

Fixation and immunostaining of Huh7.5 cells was performed using monoclonal anticore Abs (C1/C2) as described recently (25, 28, 29). Cells were embedded in fluorescence-mounting medium containing DAPI (4–6-daimidino-2-phenylindole; Vector Laboratories) for cell nuclei staining. Microscopy was performed using a fluorescent microscope (Leica). For detection of DNA fragmentation, a TUNEL assay was used as previously described (30). The percentage of apoptotic cells was determined by counting the number of TUNEL-positive cells. At least 300 cells were counted out of five microscopic fields at ×400 magnification for each experiment.

Statistical analysis

Data are expressed as means ± SEM (n = number of cell preparations). SEM was omitted in the figures when smaller than symbol size. Each experiment was performed at least in three independent cell preparations.

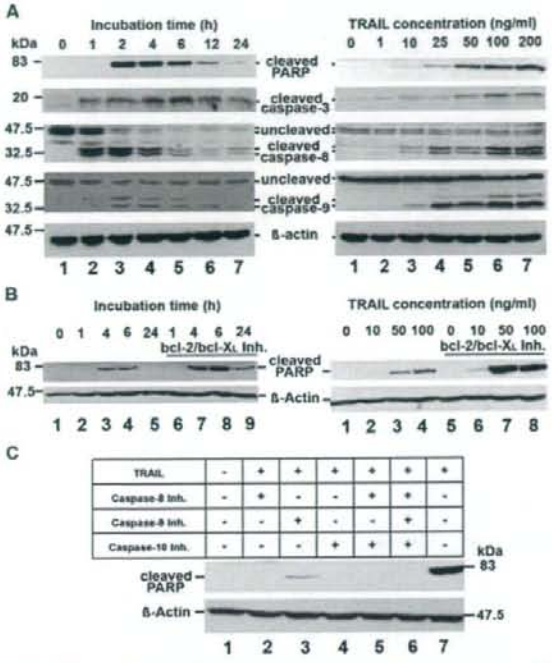

FIGURE 2. TRAIL-induced apoptosis in human Huh7.5 hepatoma cells is caspase and Bcl-2/Bcl-x_L dependent. Following incubation with TRAIL, Huh7.5 cells were lysed and protein lysates were subjected to SDS-PAGE and Western blot analysis using anti-human PARP and caspase-specific Abs. *A*, *left panel*, Time course of TRAIL-induced apoptosis with PARP-, caspase-3, caspase-8, and caspase-9 cleavage following 1–24 h incubation with TRAIL at a concentration of 50 ng/ml. *Right panel*, Dose-dependent induction of TRAIL-dependent apoptosis at TRAIL concentrations ranging from 1 to 200 ng/ml (incubation time 2 h). *B*, Mechanism of TRAIL-induced apoptosis. Huh7.5 cells were incubated with TRAIL following a 30-min preincubation with Bcl-2-, Bcl-x_L-, and caspase inhibitors. Cells were incubated at a TRAIL concentration of 50 ng/ml (*left panel*), or for 2 h with different TRAIL concentrations (*right panel*). Inhibition of anti-apoptotic Bcl-2 and Bcl-x_L using dimethoxy-dihydro-dibenzodiazocine dioxide and dimethoxy-dinitrosobenzyl (50 μmol/l) showed a marked induction of TRAIL-induced apoptosis. *C*, After 10 min preincubation time with caspase-8 and -10 inhibitors Z-IETD-FMK (20 μmol/l) and Z-AEVD-FMK (20 μmol/l), cells were incubated for 2 h at a TRAIL concentration of 50 ng/ml. The inhibition of proapoptotic caspases-8 and -10 completely abolished TRAIL induced apoptosis (*lanes 2* and *4*), whereas inhibition of caspase-9 by inhibitor Z-LEHDFMK (20 μmol/l) markedly reduced apoptosis (*lane 3*).

Results were compared using the Student's *t* test; $p < 0.05$ was considered statistically significant.

Results

TRAIL induces apoptosis in Huh7.5 hepatoma cells, the target cell line for HCV infection

Sensitivity of human hepatoma cells to induction of apoptosis has been shown to differ among various cell lines. This is illustrated by the fact that for Huh7 cells, the parental cell line of Huh7.5, apoptosis induction as well as resistance following interaction with TRAIL have been reported (31–33). Thus, we studied mechanisms of TRAIL-induced apoptosis in Huh7.5 cells, a target cell line for infectious recombinant HCVcc. As shown in Fig. 2, TRAIL rapidly and dose-dependently induced cleavage of caspase-8, -9, and -3 (Fig. 2). The amounts of cleaved and uncleaved caspase-8, caspase-9, and PARP declined during apoptosis. This decline most likely reflects degradation of these proteins due to apoptosis-activated proteases as described in many model systems for apoptosis (34–36). Caspase activation is a marker of the susceptibility of the cell to undergo apoptosis, but not equivalent to apoptosis (for review, see Ref. 9). To confirm that Huh7.5 cells indeed underwent irreversible apoptosis following TRAIL incubation, we analyzed PARP cleavage, a marker of irreversible cell death (37). After incubating Huh7.5 cells with TRAIL at a concentration of 50 ng/ml for 2 h, cleavage of PARP was detectable (Fig. 2). These data demonstrate that TRAIL induces apoptosis in Huh7.5 hepatoma cells in a dose-dependent manner.

Next, we aimed to study the mechanism of TRAIL-induced apoptosis in hepatocyte-derived cell lines. Using defined inhibitors targeting key mediators of distinct apoptotic pathways, we studied the functional impact of Bcl-2, Bcl-x_L, and caspases for TRAIL-induced cell death. Proteins belonging to the Bcl-family are important modulators of mitochondrial apoptosis (38). As shown in Fig. 2*B* specific inhibition of anti-apoptotic effectors Bcl-2 and Bcl-x_L with dimethoxy-dihydro-dibenzodiazocine dioxide and dimethoxy-dinitrosobenzyl did not result in spontaneous apoptosis in Huh7.5 cells, but enhanced TRAIL-induced apoptosis. These data indicate that TRAIL-induced apoptosis is suppressed by Bcl-2 and Bcl-x_L, but not completely inhibited. Hepatocytes belong to the so-called type-II cells that need mitochondrial amplification and consecutive caspase-9 activation for apoptosis induction via death ligands (39). In Huh7.5 cells, inhibition of caspase-9 with Z-LEHDFMK largely abolished TRAIL-induced apoptosis, as determined by cleaved PARP fragments (Fig. 2*C*, *lane 3*). Inhibition of the initiator caspases-8 and -10 with Z-IETD-FMK and Z-AEVD-FMK, completely prevented TRAIL-induced apoptosis (*lanes 2* and *4*). In contrast, inhibition of caspase-3 only marginally altered TRAIL-induced apoptosis (see Fig. 8). These data demonstrate that TRAIL-induced apoptosis in Huh7.5 cells, similar to hepatocytes, largely depends on mitochondrial amplification. Furthermore, our data indicate that TRAIL-induced apoptosis is blocked if downstream signaling of the receptor-activated death-inducing signaling complex via caspase-8/-10 is inhibited.

Replicating infectious HCV sensitizes Huh7.5 cells and primary human hepatocytes to TRAIL-induced apoptosis

Because many viruses including cytomegalovirus (40), influenza virus (41), and adenovirus (42) have been shown to sensitize infected cells to TRAIL-induced apoptosis, we aimed to study whether HCV infection sensitizes Huh7.5 cells to TRAIL-induced apoptosis. To address this issue, we first exposed Huh7.5 cells harboring replicating infectious HCV to TRAIL. Compared with control transfected cells, replicating infectious HCV RNA markedly and significantly enhanced TRAIL-induced apoptosis, as shown by cleaved PARP (Fig. 3, *A–D*) and cleaved caspase-8 and -9 (Fig. 3, *E* and *F*). At the single-cell level, the TUNEL assay showed a statistically significant enhancement of TRAIL-induced apoptosis in cells harboring replicating HCV RNA, but not in the control cells harboring replication-deficient control RNA (Fig. 3, *G* and *H*). These results demonstrate that HCV sensitizes its host cells to TRAIL-induced apoptosis.

Next, we aimed to confirm whether sensitization to TRAIL-induced apoptosis was also present in HCV-infected cells. Thus, we incubated Huh7.5 cells with HCVcc or noninfectious control supernatants derived from cells transfected with JFH1/ΔE1E2 RNA unable to produce infectious viral particles. As shown in Fig. 4, exposure of HCV-infected Huh7.5 cells to TRAIL resulted in enhanced apoptosis compared to control cells incubated with control supernatants, as shown by cleaved PARP (Fig. 4*A*). Compared

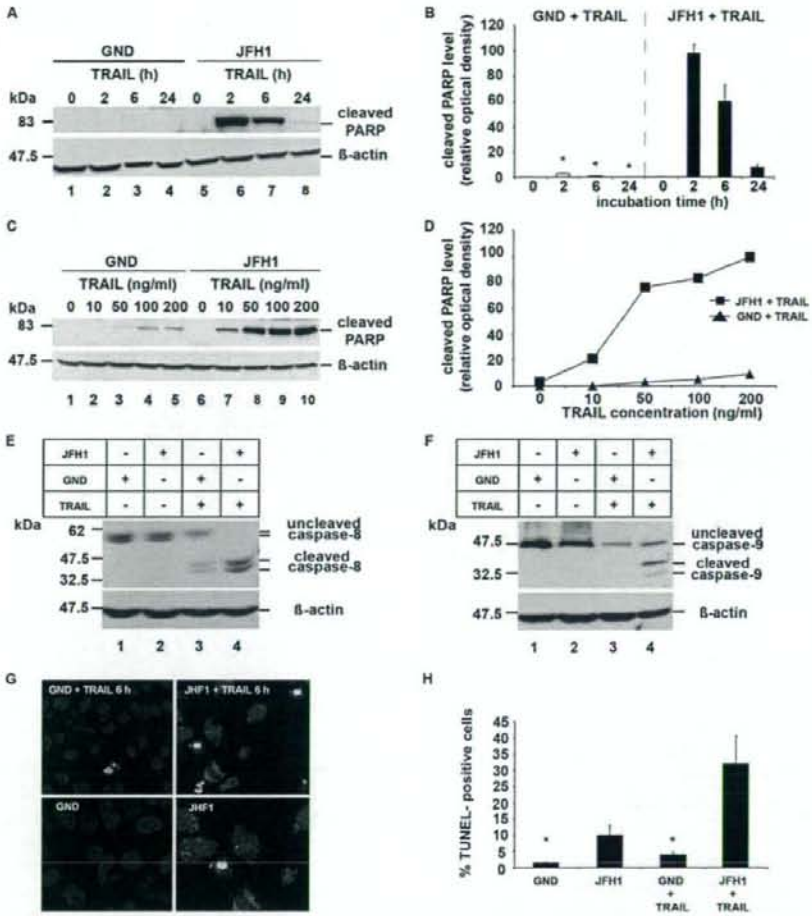

FIGURE 3. HCV replication sensitizes Huh7.5 cells to TRAIL-induced apoptosis. Huh7.5 cells were transfected with JFH1 RNA or replication-deficient control RNA (GND). Seventy-two hours later, TRAIL was added and cells were incubated for an additional time period as indicated. Following cell lysis, apoptosis was assessed by immunoblot analysis of cleaved PARP, caspase-8, -9, and TUNEL assay. *A* and *C*, Analysis of apoptosis of Huh7.5 cells by immunoblot analysis of cleaved PARP. In the experiment depicted in *A*, cells were incubated with TRAIL (50 ng/ml) for 0–24 h. In the experiment depicted in *C*, cells were incubated for 6 h with increasing concentrations of TRAIL (0–200 ng/ml). *B* and *D*, Quantification of apoptosis by optical densitometric analysis of cleaved PARP levels relative to β-actin levels. Means ± SEM from three independent experiments are shown. *E* and *F*, Analysis of apoptosis of Huh7.5 cells incubated with TRAIL (50 ng/ml) for 6 h by immunoblot analysis of cleaved caspase-8 (*E*) and caspase-9 (*F*) as described in Fig. 2. *G*, Analysis of apoptosis of Huh7.5 cells by TUNEL assay as described in *Materials and Methods*. Immunostaining of HCV core protein (red, Cy3) and TUNEL reaction (green, FITC) were performed as described in *Materials and Methods*. *H*, Quantification of TUNEL-positive cells in HCV RNA-transfected Huh7.5 cells. Data are shown as mean percentage of TUNEL-positive cells divided by all cells (n = 500 corresponding to 100%); error bars represent SEM of three independent experiments; *, statistically significant vs JFH1 (Student's t test, $p < 0.05$).

to viral genome delivery by electroporation, HCV-dependent enhancement of TRAIL-induced apoptosis appeared to be lower in HCV JFH1-infected hepatoma cells (as shown by the lower level of cleaved PARP when comparing Fig. 4*A* to 3*C*). This difference was most likely due to low levels of MOI ($TCID_{50}$ of 10^4/ml for HCVcc derived from HCV-JFH1 strain) resulting in less efficient delivery of the viral genome in infection compared with transfection experiments. To address this issue, we repeated infection experiments using infectious particles of viral strain Jc1 (J6-JFH1). In contrast to the JFH1 strain, the Jc1 isolate has been shown to allow production of virus with markedly enhanced infectivity (24). Indeed, infection of Huh7.5 cells at higher MOIs with HCV virions derived from the HCV Jc1 strain (TCID50 of 10^5–10^6/ml) resulted in similar enhancement of TRAIL-induced apoptosis as seen in transfection experiments (compare Fig. 4*C* with 3*C*).

Huh7.5 cells are derived from transformed hepatoma cells and therefore only represent a surrogate model for the natural target cell for HCV infection, the PHH. To confirm the relevance of our findings for the natural target cell of HCV infection, we reproduced key findings in HCV-infected primary human hepatocytes in contrast to Huh7.5 hepatoma cells have been shown to be resistant to TRAIL-induced apoptosis (5–7). Indeed, incubation of PHH with TRAIL did not yield in cleavage of PARP (Fig. 4*D*, *lane 4*). Whereas incubation of PHH with TRAIL did not result in apoptosis (Fig. 4*D*, *lane 5*), HCV JFH1 infection rendered PHH sensitive to TRAIL-induced apoptosis (Fig. 4*D*, *lane 2*). Infection of PHH with HCV JFH1 was confirmed by detection of HCV NS5A protein expression in infected cells using immunoblot (Fig. 4*D*, *lanes 2* and *3*). These results confirm the relevance of HCV-dependent sensitization to TRAIL-induced apoptosis for PHH.

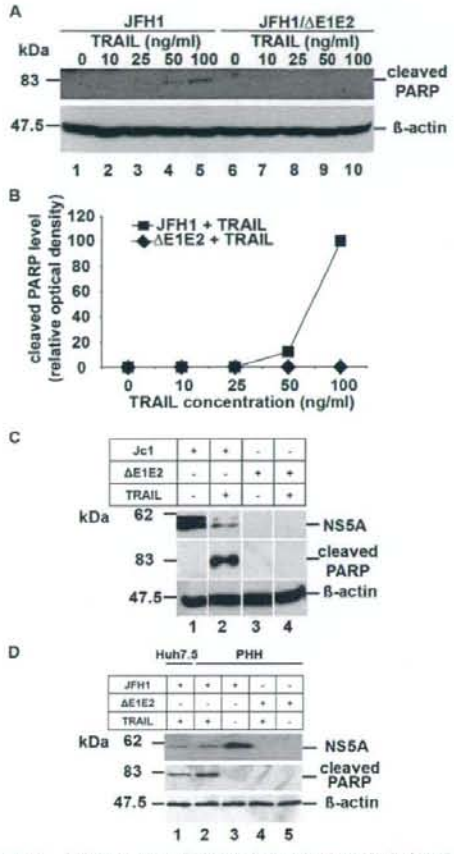

FIGURE 4. Enhancement of TRAIL-induced apoptosis during HCV infection. Infection of PHH and Huh7.5 cells with HCV JFH1 $TCID_{50}$ of 10^4/ml and HCV Jc1 $TCID_{50}$ of 10^6/ml was performed by incubation of cells for 3 h with tissue culture supernatants of JFH1, Jc1, or JFH1/ΔE1E2 transfected Huh7.5 cells as described previously (19, 22). Seventy-two hours postinfection, TRAIL was added at the concentrations indicated. Six hours following the addition of TRAIL, apoptosis was analyzed by immunoblot analysis of cleaved PARP as described in Fig. 3. HCV infection was confirmed by immunoblot analysis of HCV NS5A expression. *A*, Immunoblot analysis of cleaved PARP in JFH1 infected Huh7.5 cells vs JFH1/ΔE1E2 control cells. *B*, Densitometric analysis of cleaved PARP from three independent experiments (see Fig. 3) showed that JFH1 infection significantly enhanced TRAIL-induced apoptosis as compared with incubation with noninfectious control supernatants (JFH1/ΔE1E2). *C*, Immunoblot analysis of cleaved PARP in Jc1-infected Huh7.5 cells vs JFH1/ΔE1E2 control cells. Cells were incubated in presence or absence of 100 ng/ml TRAIL for 2 h. *D*, Immunoblot analysis of cleaved PARP in JFH1-infected PHH and Huh7.5 vs JFH1/ΔE1E2 control cells. TRAIL (50 ng/ml, 6 h) induced cleavage of PARP only in HCV infected PHH (*lane 2*), but not in JFH1/ΔE1E2 control (*lane 4*). *, Statistically significant using Student's *t* test ($p < 0.05$).

Interestingly, we observed that transfection of Huh7.5 cells with replication-competent full-length HCV RNA itself can result in apoptosis of Huh7.5 cells as indicated by an increase in the number of TUNEL-positive cells compared with control cells (Fig. 3*H*) and a low-level induction of cleaved PARP using immunoblots with long exposure times (see Fig. 8*B*, *lane 2* and data not shown). However, the induction of apoptosis by the virus itself was less pronounced when compared with apoptosis after exposure to

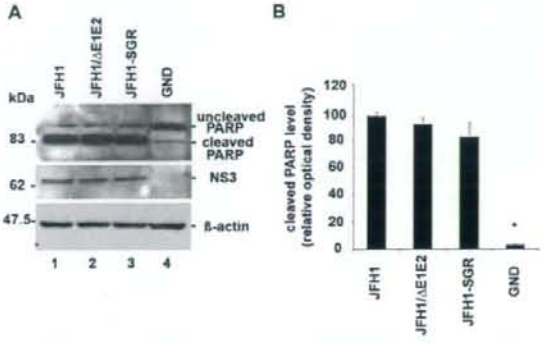

FIGURE 5. Enhancement of TRAIL-induced apoptosis during HCV infection is independent of HCV structural protein expression and viral RNA. *A*, Huh7.5 cells were transfected with HCV JFH1 RNA derived from constructs described in Fig. 1. Seventy-two hours following transfection, cells were exposed to TRAIL at a concentration of 50 ng/ml for 2 h and apoptosis was analyzed as described in Fig. 3. *B*, Densitometric analysis of cleaved PARP (see Fig. 3) from three independent experiments indicated a similar enhancement of TRAIL-apoptosis by JFH1 full-length and subgenomic replicons.

TRAIL in cells harboring replicating HCV (compare *lanes 1* and *5* in Fig. 4*A*; *lanes 2* and *4* in Fig. 3, *E* and *F*; *lanes 2* and *4* see in Fig. 8*B*).

Enhancement of TRAIL-induced apoptosis is mediated by HCV nonstructural proteins

To identify the viral factor(s) enhancing TRAIL-induced apoptosis, we determined whether HCV structural protein expression is required for HCV-TRAIL interaction. To address this question, we transfected Huh7.5 cells with a JFH1 variant (JFH1/ΔE1E2) containing a deletion in the HCV envelope coding region preventing synthesis of infectious viral particles. Because the phenotype of full-length JFH1 RNA and JFH1/ΔE1E2 was indistinguishable in regard to enhancement of TRAIL-induced apoptosis (Fig. 5), we conclude that HCV-TRAIL interaction is independent of production of infectious viral particles. To determine whether structural proteins are required for HCV-enhanced TRAIL-induced apoptosis, we compared the full-length JFH1 RNA with a JFH1 subgenomic replicon lacking the HCV core-NS2 region. Because the JFH1 subgenomic replicon exhibited a similar apoptosis phenotype as full-length JFH1 RNA (Fig. 5), we conclude that the expression of HCV structural proteins and NS2 is not required for enhancement of TRAIL induced apoptosis and sensitization to TRAIL-induced apoptosis is mediated predominantly by the HCV nonstructural proteins.

HCV JFH1-dependent enhancement of TRAIL-induced apoptosis is caspase-9 dependent

Following mapping the viral factors required for HCV-dependent enhancement of TRAIL-induced apoptosis, we investigated the cellular factors mediating this HCV-host interaction. Several studies pointed to an involvement of TRAIL in apoptosis of virus-infected hepatocytes by an autocrine loop (43, 44). To address this question, we studied the impact of HCV replication and protein expression on the expression of TRAIL and TRAIL receptor R1 in Huh7.5 cells. As shown in Fig. 6, cells harboring replicating infectious HCV RNA showed decreased expression levels of TRAIL and unchanged levels of TRAIL receptor R1 expression when compared with cells transfected with replication-deficient viral

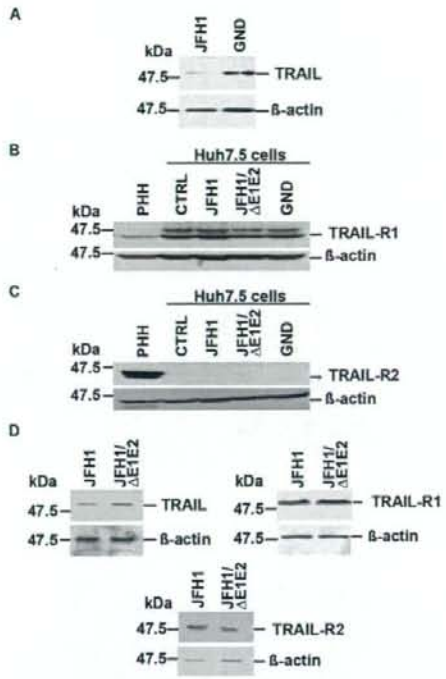

FIGURE 6. JFH1-induced apoptosis in primary human hepatocytes and Huh7.5 cells is independent of TRAIL and TRAIL-R1/-R2 expression. PHH and Huh7.5 cells were infected/transfected with virions/RNA derived from constructs depicted in Fig. 1. Seventy-two hours postinfection/transfection, TRAIL, TRAIL-receptor R1, and TRAIL-receptor R2 expression were analyzed by Western blot analysis using specific Abs directed against human TRAIL, TRAIL-R1, and TRAIL-R2. *A*, Transfection of Huh7.5 cells with JFH1 RNA resulted in suppression of TRAIL expression, as compared with Huh7.5 cells transfected with replication-deficient GND RNA. *B* and *C*, Absent modulation of TRAIL-R1 expression and lacking TRAIL R2 expression in HCV JFH1 transfected Huh7.5 cells. Immunoblot analyses of naive PHH are shown as positive controls for TRAIL-R1 and TRAIL-R2 expression (*lane 1*). *D*, Down-regulation of TRAIL expression in PHH infected with HCV JFH1. Expression of TRAIL-R1 and TRAIL-R2 in PHH infected with HCV JFH1.

control RNA. In contrast to PHH, TRAIL receptor R2 was not expressed in Huh7.5 cells (Fig. 6*C*). Similar to Huh7.5 cells, infection of PHH with HCV JFH1 neither increased TRAIL expression, nor enhanced protein expression of TRAIL receptors R1, respectively (Fig. 6*D*). These data suggest that a TRAIL autocrine loop does not play a major role for TRAIL-induced sensitization in this HCV infectious tissue culture system.

The mitochondrial apoptosis pathway has been shown to play an important role in virus-induced modulations of host cell apoptosis (10). As shown in Fig. 2, we have already demonstrated that TRAIL-induced apoptosis in Huh7.5 cells is enhanced following the inhibition of Bcl-2/Bcl-x_L (Fig. 2*B*). We therefore analyzed Bcl-2 and Bcl-x_L protein expression in JFH1-transfected Huh7.5 cells and JFH1 infected PHH. Interestingly, expression of Bcl-2 and Bcl-x_L was suppressed in JFH1-transfected Huh7.5 cells (Fig. 7, *A* and *B*). These results were confirmed in PHH, where infection with JFH1 appeared to reduce Bcl-2 and Bcl-x_L protein expression (Fig. 7*C*). The less pronounced reduction in Bcl-2/Bcl-x_L protein expression observed in PHH (Fig. 7*C*) compared with Huh7.5 cells (Fig. 7, *A* and *B*) may be due to the lower number of cells con-

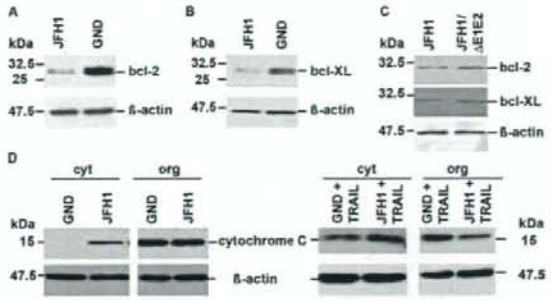

FIGURE 7. HCV JFH1 replication suppresses antiapoptotic Bcl-2 and Bcl-x_L expression. Huh7.5 cells and PHH were transfected/infected with HCV RNA/virions derived from constructs depicted in Fig. 1. Seventy-two hours post transfection, Bcl-2 (*A* and *C*), Bcl-x_L (*B* and *C*) expression and cytochrome C levels in cellular subfractions (*D*) were analyzed by Western blot analysis. Suppression of antiapoptotic Bcl-2 (*A*) and antiapoptotic Bcl-x_L (*B*) protein expression in JFH1-transfected Huh7.5 cells compared with Huh7.5 cells transfected with replication-deficient HCV GND RNA was detectable. *C*, Bcl-2 and Bcl-x_L protein expression in PHH infected with HCV JFH1. PHH were infected with HCV JFH1 as described in Fig. 4 and Bcl-2 and Bcl-x_L protein expression was detected 72 h following infection as described above. *D*, Cytochrome C levels in subcellular fractions (cytosolic and organelle fractions containing mitochondria) of cells with replicating virus incubated with or without TRAIL. Cells were transfected with JFH1 RNA or replication-deficient control RNA (GND). Seventy-two hours post transfection TRAIL was added (100 ng/ml) for 2 h. Following lysis and cellular fractionation of cell lysates as described in *Materials and Methods*, cytochrome C levels in cellular subfractions were analyzed by immunoblot using anti-cytochrome C specific Ab. Cyt, cytosolic subfraction; Org, organelle subfraction containing mitochondria.

taining replicating HCV in PHH. Incubation of Huh7.5 with a Bcl-x_L mimetic peptide resulted in a small but reproducible reduction (three of three experiments) of TRAIL-induced apoptosis in JFH1 replicating cells (Fig. 8*D*). Mitochondrial-dependent apoptosis is characterized by release of mitochondrial cytochrome C into the cytoplasm (11, 12). We therefore studied cytochrome C levels in cytosolic fractions and fractions containing the mitochondria of HCV JFH1-replicating Huh7.5 cells incubated with TRAIL. As shown in Fig. 7*D*, hepatoma cells with replicating virus and treated with TRAIL demonstrated an increase of cytochrome C levels in cytosolic fractions compared with control-transfected cells incubated with TRAIL. These data suggest that cytochrome C appears to be released from the mitochondria in TRAIL-treated cells with replicating HCV and suggests that the mitochondrial pathway contributes to HCV-induced enhancement of TRAIL-induced apoptosis. Interestingly, HCV replication alone also resulted in release of cytochrome C into the cytosol (Fig. 7*D*) consistent with low level induction of apoptosis by JFH1 itself (see Fig. 3*H*).

Next, we aimed to study the impact of caspases for HCV-mediated enhancement of TRAIL-induced apoptosis. Several forms of apoptosis do not involve caspase activation. We therefore inhibited caspases with the pan-caspase inhibitor Z-VAD-FMK. Interestingly, inhibition of caspases completely abolished JFH1-dependent enhancement of TRAIL-induced apoptosis (Fig. 8*A*, *lane 3* and Fig. 9*C*, *lane 3*). These findings indicate an essential role of caspase activation for TRAIL-induced apoptosis of Huh7.5 cells harboring replicating HCV. To determine the impact of mitochondrial apoptosis in HCV infection, we inhibited the mitochondrial-activated caspase-9. Inhibition of caspase-9 with Z-LEHD-FMK largely blocked JFH1-dependent enhancement of TRAIL-induced apoptosis (Fig. 8*B*, *lane 5*), suggesting an essential contribution of the mitochondrial apoptotic pathway for

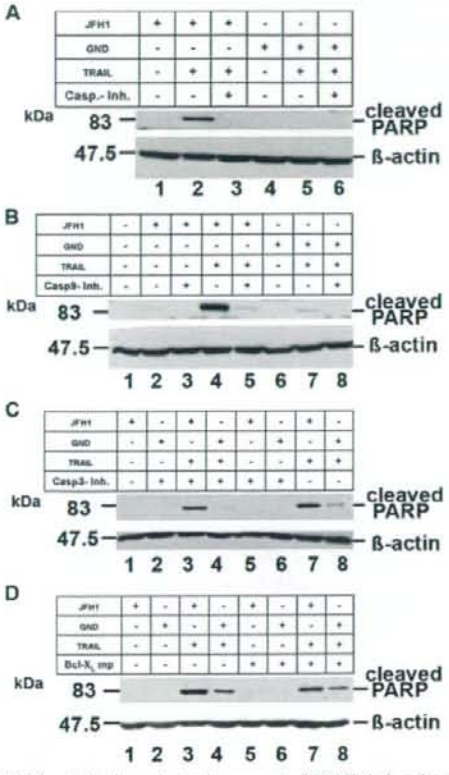

FIGURE 8. JFH1-dependent enhancement of TRAIL-induced apoptosis is caspase-9 dependent. Huh7.5 cells were transfected with HCV JFH1 or control GND RNA as described in Fig. 3. 72 h following transfection, cells were exposed to TRAIL in the presence or absence of caspase-inhibitors (see Fig. 2) and apoptosis was analyzed as described in Fig. 2. *A*, JFH1-dependent enhancement of TRAIL-induced apoptosis was completely inhibited by preincubation with pan-caspase inhibitor Z-VAD-FMK (Casp-Inh., 20 μM). *B*, JFH1-dependent enhancement of TRAIL-induced apoptosis was blocked by caspase-9 inhibitor Z-LEHD-FMK (Casp-9 Inh., 20 μM; *lane 5*), whereas JFH1-dependent enhancement of TRAIL-induced apoptosis (*lane 4*) was reduced by caspase-9 inhibitor to the level of JFH1 induced apoptosis (*lane 2*). *C*, Inhibition of caspase-3 using a caspase 3 inhibitor (2-(4-Methyl-8-(morpholin-4-ylsulfonyl)-1,3-dioxo-1,3-dihydro-2H-pyrrolo[3,4-c]quinolin-2-yl)ethyl- acetate; 10 μM) only marginally modified JFH1/TRAIL induced apoptosis as determined by analysis of cleaved PARP fragment. *D*, Preincubation of JFH-1 transfected Huh7.5 cells with Bcl-x_L mimetic peptide (100 nM, 60 min) resulted in a minor reduction of TRAIL-dependent induction of apoptosis, as determined by analysis of cleaved PARP fragment.

HCV-mediated sensitization of TRAIL-induced apoptosis. Interestingly, inhibition of caspase-3 only marginally affected TRAIL-induced apoptosis in JFH1 replicating Huh7.5 cells (Fig. 8*C*) indicating that caspase-3 does not play a major role in execution of TRAIL/HCV apoptosis.

TRAIL-induced apoptosis in HCV target cells results in down-regulation of viral protein expression

If HCV replication enhances TRAIL-induced apoptosis, HCV-infected cells should preferentially be eliminated. To address this question, we studied the impact of TRAIL on HCV protein expression in Huh7.5 cells and PHH harboring replicating infectious HCV. In line with this hypothesis, incubation of HCV JFH1 RNA-

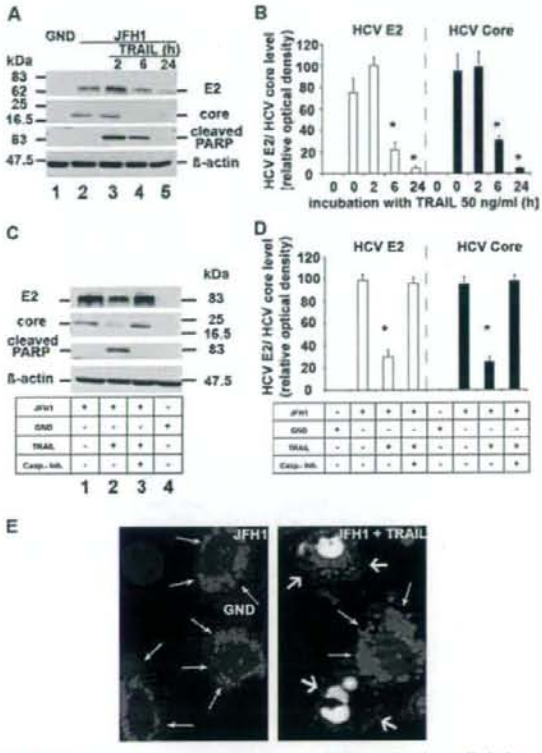

FIGURE 9. TRAIL-induced apoptosis in HCV-replicating cells induces down-regulation of viral protein expression. Huh7.5 cells were transfected with HCV JFH1 or control GND RNA as described in Fig. 2. Seventy-two hours following transfection, cells were exposed to TRAIL in the presence or absence of the pan-caspase inhibitor Z-VAD-FMK (Fig. 2) and apoptosis was analyzed as described in Fig. 2. HCV core and E2 protein expression were analyzed by immunoblot. *A*, TRAIL (50 ng/ml) induces apoptosis as shown by cleaved PARP and results in down-regulation of HCV core and E2 protein expression. TRAIL incubation time is indicated above the lanes. *B*, Densitometric analysis of HCV core and E2 levels demonstrated statistically significant reduction of HCV core and E2 protein expression 6 and 24 h following incubation with TRAIL, respectively. *C* and *D*, Inhibition of TRAIL-induced apoptosis by preincubation with pan-caspase-inhibitor Z-VAD-FMK (20 μmol/l) restores HCV E2 and core protein expression as shown by immunoblot (*C*) and densitometric analysis of HCV core and E2 protein levels (*D*). Data are presented as mean values of three independent experiments $\pm$ SEM. *, Statistically significant using Student's t test, $p < 0.05$. *E*, Analysis of HCV protein expression in apoptotic cells by immunofluorescence. Huh7.5 cells were transfected with JFH1 RNA as described in Fig. 1 stained with a monoclonal anti-HCV core Ab (red) and counterstained with DAPI (blue) for visualization of cell nuclei. Apoptosis was determined by TUNEL assay (green) as described in *Materials and Methods*. Single cell analysis using confocal laser scanning microscopy revealed reduced HCV core expression levels in apoptotic Huh7.5 cells compared with nonapoptotic cells expressing HCV proteins. Cells with replicating HCV without apoptosis are indicated by long, thin arrows, apoptotic (TUNEL positive) cells with replicating HCV are indicated by short, thick arrows.

transfected Huh7.5 cells with TRAIL induced a significant reduction of HCV core and E2 protein expression (Fig. 9, *A* and *B*). As shown in immunofluorescence analyses of individual cells, apoptotic Huh7.5 cells with replicating HCV exhibited a marked reduction of HCV core protein expression compared with nonapoptotic cells (Fig. 9*E*). These results were further confirmed by

quantification of viral protein expression using immunofluorescence analyses (data not shown). Similar to findings in Huh7.5 hepatoma cells, incubation with TRAIL appeared to result in suppression of HCV protein expression in HCV JFH1-infected PHH (Fig. 4*D*, *lane 2*, compared with *lane 3*). The TRAIL-dependent reduction of HCV protein expression was dependent on apoptosis induction, since preincubation of Huh7.5 cells with pan-caspase-inhibitor Z-VAD-FMK completely restored expression of the HCV proteins core and E2, respectively (Fig. 9, *C* and *D*). These findings confirm the impact of TRAIL-induced apoptosis for HCV-host interactions and suggest that sensitization to TRAIL-induced apoptosis in cells harboring replicating HCV may contribute to control of HCV infection.

Discussion

In this study, we demonstrate that HCV infection sensitizes the host cell to TRAIL-induced apoptosis. Detailed analyses indicate that this sensitization depends on the expression of HCV nonstructural proteins NS3, NS4, and NS5. The interaction between HCV and the host cell apoptosis machinery involves caspase-9 and the mitochondrial but not the autocrine TRAIL-mediated pathway. Furthermore, we show that induction of apoptosis by TRAIL results in suppression of HCV protein expression, suggesting that this mechanism may contribute to elimination of HCV-infected hepatocytes.

Viral factors required for sensitization to TRAIL-induced apoptosis

For virtually all HCV proteins, interference with apoptosis has been reported. However, most studies assessing the effect of HCV infection on cellular apoptosis were performed in surrogate models of HCV infection, e.g., stably transfected cell lines or recombinant proteins expressed in heterologous systems. Thus, the relevance of these observations for HCV infection remained uncertain. Limitations of surrogate models of HCV infection are, among others, artificially elevated levels of expressed HCV proteins or the lack of genetic elements in subgenomic replicons (13). To overcome these limitations and to study the mechanism of apoptosis in a model system closer to HCV infection in vivo, we used the HCVcc model system allowing us to study HCV-host interactions in the context of the complete viral life cycle (18–20).

In contrast to our observations having identified the HCV nonstructural proteins as key players for sensitization of TRAIL-induced apoptosis, a recent study had demonstrated an important role of core for TRAIL-induced apoptosis (31). Isolate-specific factors (genotype 1 vs 2), different core protein levels in the infectious cell culture system (this study), and transfection of cDNA (31), as well as a dominant effect of nonstructural proteins in the infectious tissue culture system, may explain the different findings. Using a full-length replicon expressing all viral proteins, Lee et al. showed that HCV envelope glycoprotein E2 can antagonize the proapoptotic effects of HCV core protein (32). In our study, we did not observe a markedly altered induction of apoptosis in cells transfected with HCV RNA containing a deletion in the HCV envelope proteins (JFH1/ΔE1E2) compared with infectious HCV RNA (Fig. 5). Because subgenomic replicons still showed sensitization to TRAIL-induced apoptosis (Fig. 5), our findings clearly demonstrate that the HCV structural proteins may not represent the major factors that determine sensitization to TRAIL, although we cannot exclude a modulatory role of these proteins. Because subgenomic replicons lack a functional NS2 protein (Fig. 1), our data also suggest that the recently described antiapoptotic effect of NS2 in a transgenic mouse model (45) may not play a major role in the enhancement of TRAIL-induced apoptosis in HCV-infected human hepatoma cells.

Interestingly, proapoptotic effects of HCV nonstructural proteins NS3/NS4A (46, 47) and NS5A (48) have been described recently. NS3 complexed with NS4A is known to translocate to the mitochondrial membrane where direct apoptosis induction, independent from caspase-8 activation can occur (47). Conversely, NS3 has been described to cleave Cardif and thereby act antiapoptotically (49). NS5A has recently been shown to directly inhibit proapoptotic Bin1, a tumor suppressor protein with a SH3 domain, thereby facilitating apoptosis induction in hepatoma cells (48). By contrast, NS5A has sequence homologies with Bcl-2 and binds to FKBP38, thereby augmenting the antiapoptotic effect of Bcl-2 (50) and inhibiting the proapoptotic action of Bax in hepatoma cells (51). Although we cannot exclude a functional relevance of antiapoptotic properties of NS5A and NS3, our data suggest that these effects are not able to override the proapoptotic effects of the HCV nonstructural proteins mediating sensitization to TRAIL.

Mechanism of HCV-induced apoptosis: impact of host cell factors

The proapoptotic effects of both NS3/NS4A (47) and NS5A (48) have been described to converge at the level of the mitochondria and may explain the proapoptotic properties of HCV infection. In this study, we demonstrate evidence that HCV-induced enhancement of Huh7.5 cell apoptosis depends on the mitochondrial pathway, because HCV replication induced cytochrome C release into the cytosol (Fig. 7*D*) and inhibition of caspase-9 markedly abolished HCV-dependent TRAIL-induced apoptosis (Fig. 8). The cytochrome C release may be partly due to the HCV-induced down-regulation of Bcl-2 and Bcl-x_L expression (Fig. 7, *A–C*). Furthermore, preincubation with a Bcl-x_L mimetic peptide resulted in a small but reproducible (three of three experiments) reduction of HCV-dependent apoptosis as shown in Fig. 8*D*. Bcl-2 and Bcl-x_L are known to be essential in inhibiting mitochondrial apoptosis (12). In line with these results, a recent study demonstrated down-regulation of antiapoptotic Bcl-2 and up-regulation of proapoptotic PUMA and Bax in freshly prepared liver sections of HCV-infected patients (5). HCV nonstructural proteins have been shown to induce ER stress (52), and Bcl-2-/Bcl-x_L-dependent transmission of ER-stress into a mitochondrial apoptotic signal has recently been demonstrated (38). Nevertheless, down-regulation of Bcl-2 and Bcl-x_L alone seems not sufficient to explain proapoptotic properties of HCV JFH1, as inhibition of both proteins did not enhance TRAIL-induced apoptosis to the extent of the HCV-dependent apoptosis (Fig. 2), and incubation of cells with a Bcl-x_L mimetic peptide was only partially modulating TRAIL-induced apoptosis in Huh7.5 cells (Fig. 8*D*).

Several authors have postulated an autocrine TRAIL-dependent apoptosis of hepatocytes. Mundt et al. (43) demonstrated TRAIL-dependent apoptosis in hepatocytes using an adenoviral vector expressing TRAIL, and Volkmann et al. (5) described an up-regulation of TRAIL receptors in HCV-infected human liver sections. Most recently, HCV-dependent up-regulation of TRAIL and apoptosis induction in a novel hepatoma cell line has been described (44). In the latter study, apoptosis of hepatoma cells was dependent on autologous TRAIL expression and HCV-dependent apoptosis resulted in death of all infected cells. In contrast, in PHH and Huh7.5 cells harboring replicating HCV, we observed a decreased expression of TRAIL and unchanged TRAIL receptor expression levels (Fig. 6). Moreover, immunohistochemistry of TRAIL expression in the HCV-infected liver revealed that nonparenchymal mononuclear cells, but not hepatocytes, appear to be predominant producers of TRAIL (data not shown). Taken together, these data